SENSING OF IMPEDANCE CARDIOGRAM USING A DIGITAL SYNCHRONOUS DEMODULATOR

A dissertation submitted in
partial fulfillment of the requirements for the degree of

Master of Technology

by

Hitendra Sahu
(113300017)

under the supervision of

Prof. P. C. Pandey

Biomedical Engineering Group
Department of Biosciences and Bioengineering
Indian Institute of Technology Bombay

June 2013

Indian Institute of Technology Bombay

M.Tech. Dissertation Approval

This dissertation entitled **"Sensing of impedance cardiogram using a digital synchronous demodulator"** by **Hitendra Sahu** (Roll No. **113300017**) is approved, after the successful completion of *viva voce* examination, for the award of the degree of **Master of Technology** in **Biomedical Engineering**

Supervisor	....	(Prof. P. C. Pandey)
Examiners	....	(Prof. L.R. Subramanyan)
	....	(Prof. V Rajbabu)
Chairperson	....	(Prof. Joseph John)

Date: 28th June 2013

Place: Mumbai

Declaration

I declare that this written submission represents my ideas and my own words and where other's ideas or words have been included, I have adequately cited and referenced the original sources. I also declare that I have adhered to all principles of academic honesty and integrity and have not misrepresented or fabricated or falsified any idea/data/fact/source in my submission. I understand that any violation of the above will be cause for disciplinary action by the institute and can also evoke penal action from sources which have thus not been properly cited or from whom proper permission has not been taken when needed.

Date: 28-06-13 Hitendra Sahu

Place: Mumbai Roll No. : 113300017

Hitendra Sahu / Prof. P. C. Pandey (Supervisor), "Sensing of impedance cardiogram using synchronous demodulation", *M. Tech. dissertation*, Biomedical Engineering Group, Department of Biosciences and Bioengineering, Indian Institute of Technology Bombay, June 2013.

ABSTRACT

Impedance cardiography is a noninvasive technique that measures variation in the thoracic impedance and relates it to the volumetric changes in the thorax during the cardiac cycle and can be used to estimate hemodynamic parameters like stroke volume and cardiac output. An impedance cardiograph consists of an alternating current source of high frequency and low amplitude, an amplifier to sense the resulting amplitude modulated voltage, a demodulator to detect the impedance signal, a baseline correction circuit, and an ECG extractor for reference purpose. Project objective is to develop a system for sensing the basal value and time-varying component of the impedance waveform, with settable excitation frequency and with very low noise and demodulation related distortions. In the present design, a microcontroller and an impedance converter chip are used for stable sinusoidal source with programmable frequency control and a digital synchronous demodulation. For current excitation, a voltage-to-current converter with balanced outputs is designed using two operational transconductance amplifiers. The sensed voltage is added with a sinusoidal voltage obtained from the excitation source and with digitally controlled amplitude and polarity to increase its modulation index before digital synchronous demodulation and for baseline correction of the sensed impedance signal. Two digital potentiometers have been used to provide independent control over current excitation and baseline correction. Synchronous digital demodulation in the impedance converter chip gives real and imaginary part of the impedance. An isolated RS232 interface along with a PC-based graphical user interface is provided to set the parameters and to acquire the sensed impedance signal.

CONTENTS

LIST OF FIGURES AND TABLES

Chapter 1
INTRODUCTION

1.1 Background

Impedance offered by biological materials is known as bioimpedance. Blood, muscle, and other tissues have different resistivities [1]. Many physiological parameters of the body can be measured noninvasively by impedance measurement. Out of the different body tissues, blood has lower resistivity, which is 130–160 $\Omega\cdot$cm and about half of that of the muscle tissue [2]. The variation in impedance across the thorax is mainly caused by the variation in the volume of blood contained within this segment of the chest. If a current is passed through the thorax then the voltage changes measured across a pair of electrodes are proportional to the impedance changes in the thorax which is caused by the movement of blood volume during cardiac cycle.

Impedance cardiography is a noninvasive technique that measures variation in the thoracic impedance and relates it to the volumetric changes in the thorax during the cardiac cycle. It can be used for estimating hemodynamic parameters like stroke volume, cardiac output, and thoracic fluid content at every heartbeat. In this technique, a high frequency and low amplitude current is injected into the thorax using a pair of electrodes placed at root of the neck and base of the thorax, and the resulting amplitude modulated voltage across the thorax is sensed using same or another pair of electrodes [3], [4]. The amplitude modulation occurs because of the variation in the thoracic impedance which is mainly caused by inflow of the blood into the aorta during each cardiac cycle [4]. The voltage signal is demodulated to extract the variation in the thoracic impedance and is processed to estimate the stroke volume and the cardiac output from these variations. These parameters may be useful in the diagnosis of the cardiac disorders. The impedance measurement is carried out at frequency of 20-150 kHz and using current excitation of less than 5 mA (rms) to avoid any risk of physiological effects [3]. In this frequency range the impedance is almost resistive in nature.

1.2 Project objective

The impedance cardiograph hardware consist of a current source, a voltage sensing amplifier, demodulator, baseline restoring circuit, a differentiator and an ECG extraction circuit. The project objective is to develop instrumentation for impedance cardiography by modification in the existing designs and exploring use of new circuits for signal acquisition and demodulation, to improve the sensitivity of the measurement, for improving noise rejection, digital synchronous demodulation used. A circuit is devised to increase the effective modulation index before demodulation in order to increase the dynamic range of the measurement and to serve as baseline correction. For calibration and testing of the ICG instrument, an impedance simulator is also developed.

A circuit based on impedance converter chip “Analog Devices AD5933” has been developed. This chip has a DDS core to generate a sinusoidal waveform and has a digital synchronous demodulator that gives the real and imaginary part of the complex impedance. DDS based sinusoidal excitation provides high amplitude stability. The chip is designed for impedance measurement by applying voltage excitation across the unknown impedance and sensing the resulting current through it. Additional circuit is devised to use this chip for measurement using current excitation and voltage sensing. A V-to-I converter is designed by using OTAs to get a balanced current output, which eliminates the need of a transformer. A baseline restoration circuit is implemented before the demodulation for improving the SNR and modulation index. Microcontroller “Microchip PIC24FJ64GB004” is used for all the control and signal acquisition operations: setting the frequency and current excitation, sensitivity setting, and baseline tracking and restoration. The circuit is battery powered and can also be powered through USB. An isolated RS232 interface is provided for setting the measurement parameters from the user interface on a PC to the microcontroller and for acquisition of the sensed signal.

1.2 Dissertation outline

Chapter 2 deals with the basics of impedance cardiography. Chapter 3 describes thoracic impedance simulator used for objective testing of the impedance cardiograph circuit. Impedance cardiograph hardware design and the new circuit approach are presented in Chapter 4. Testing procedure and the results are given in the fifth chapter. Chapter 6 gives a summary of the project, and some suggestions for taking the development forward. Supplementary information on the design is provided in the appendices.

Chapter 2
IMPEDANCE CARDIOGRAPHY

2.1 Background

Impedance cardiography is a noninvasive method for determining the stroke volume and thereby cardiac output. Stroke volume (SV) is the volume of blood ejected by the left ventricle in each heartbeat. Cardiac output is defined as the volume of the blood ejected by the left ventricle every minute. It can be calculated by multiplying stroke volume with the heart rate.

Impedance cardiography is based on the principle of variations in the thoracic impedance during ventricular ejection period. This pulsatile change in the impedance is primarily due to the cardiovascular activity. Approximately half of this impedance change is related to the volumetric changes of the blood in the arteries [2]. The remaining impedance change is due to the variation of the specific resistivity of the blood as a function of blood velocity, which is related to the alignment of the erythrocytes [2]. Respiration also causes time-varying impedance changes in the thoracic region and these impedance changes are related to the varying amount of the air in the lungs [2]. The impedance change due to cardiovascular activity is used in the calculation for quantification of cardiac output, while the impedance change due to the respiration is an artifact which must be removed to obtain the accurate results [5].

The blood pumped out by the heart into the thorax during each cardiac cycle reduces the thoracic impedance as the blood flowing in the aorta provides a low impedance part for the injected current. The impedance variation is sensed by injecting a current of high frequency and low amplitude through the thorax and sensing the voltage generated across it. The sensed voltage is demodulated to extract the amplitude variations from which the stroke volume can be calculated. Thoracic impedance is measured at the frequency range of 20 - 150 kHz and using current of less than 5 mA rms, to reduce the risk of physiological effects [3], [6]. The frequency range is selected to minimize electrode polarization problems and low current density is selected to avoid tissue damage mainly due to heating effects. The lower frequency limit of 20 kHz is imposed to easily isolate the voltage caused by excitation from the other bioelectric signals such as ECG and EMG, for reducing the variations in contact impedance of the electrodes, and for the effective suppression of the carrier ripple in the demodulated output [3]. The upper frequency limit is selected because measurement at higher frequencies gets affected by parasitic impedance and the current path may not include the deeper thoracic regions. The impedance is almost resistive in this frequency range and the phase difference between the injected current and the sensed voltage is very less and can be neglected. The thoracic impedance comprises of two parameters. One is the basal impedance due to the lungs, tissue, bone, muscle, etc., which remain unchanged with time. The second parameter is the pulsatile impedance change which varies periodically with each cardiac cycle. The normal range of basal impedance is 20 – 200 Ω and the variations in the impedance lie in the range of about 0.2 Ω of the basal impedance [4].

2.2 ICG Waveform, model, and equations

Impedance waveform itself does not have a good correlation with the ECG waveform, but its negative first derivative shows a fair correlation with the ECG waveform. Thus negative first derivative of the impedance waveform is considered to be a useful signal and is known as the impedance cardiogram [7]. Figure 2.1 shows typical impedance waveform, impedance cardiogram and ECG waveform. Different points marked on the ICG waveforms are related to the various cardiac activities. Point A shows the downward deflection due to the contraction of the atria, and B represents the start of ejection of blood by the left ventricle thus correlated with the aortic valve opening, point C represents upward deflection occurring during systole due to increased blood flow into the aorta, and X point coincides with the closure of the aortic valve, O point shows the diastolic upward deflection, and the maximum point coincides with the mitral valve opening snap [7] [8]. LVET is the left ventricular ejection time (s) and $-(dZ/dt)_{\max}$ is the maximal impedance change during systole (Ω/s). These two indices LVET and $-(dZ/dt)_{\max}$ from the ICG waveform are used in most of the methods for stroke volume calculation.

A parallel column model [4] is used to relate volumetric changes to the impedance change during systole. The thorax is modeled as consisting of a cylinder, constant impedance Z_0 connected in parallel with a cylindrical column with a variable impedance having a uniform cross-sectional area A, length L, and known resistivity ρ, as shown in Figure 2.2. As the cross-sectional area of the cylinder varies from zero to a finite value, the maximum change in the impedance ΔZ and the maximum change in the volume ΔV can be related as [4].

$$\Delta V = \left(\rho L^2 / Z_0^2\right) \Delta Z \tag{2.1}$$

This model assumes that there is no outflow of the blood from the thorax during systole and the volume of the variable impedance column is zero before systole. A forward extrapolation technique is used to account the blood that leaves the thorax during later part of the systole [4]. The modified form of the equation, also known as Kubicek's equation [4] is given as,

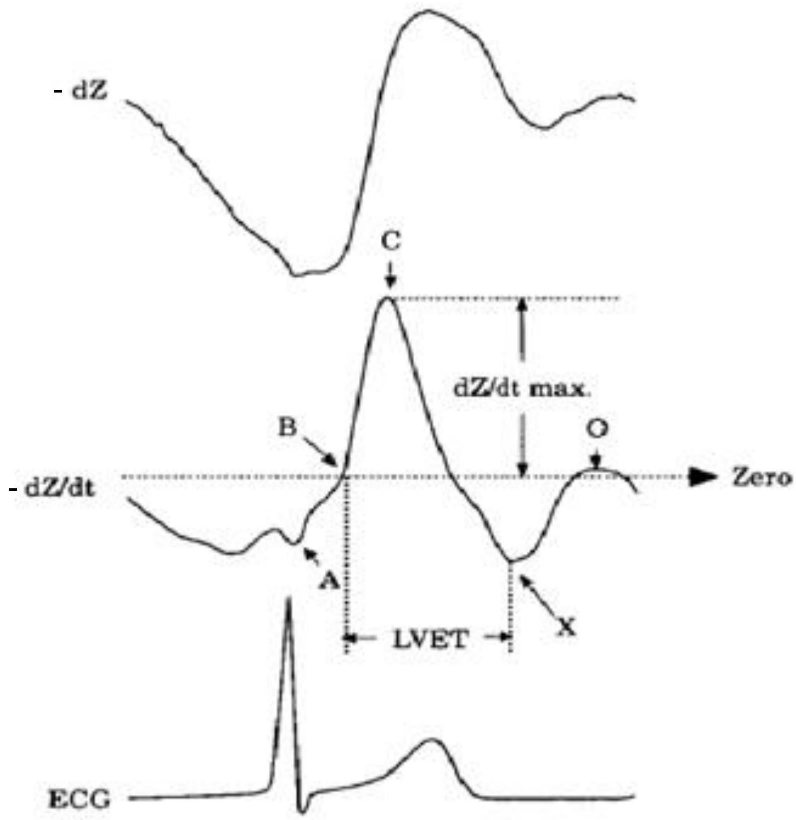

Figure 2.1 Typical -dZ, -dZ/dt, and ECG waveforms [7]

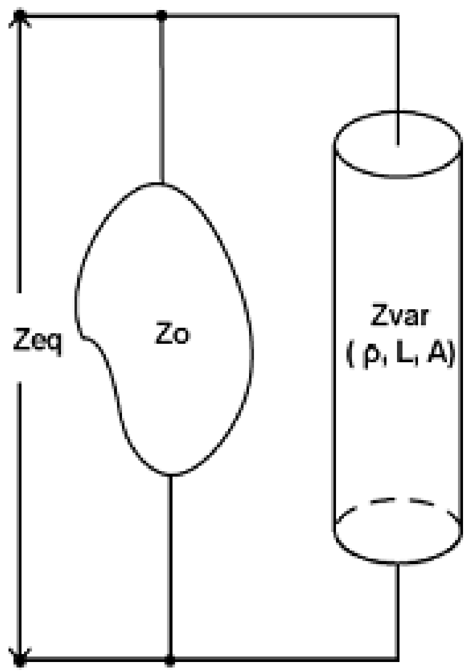

Figure 2.2 Parallel column model [4]

$$\Delta V = \left(\frac{\rho L^2}{z_0^2}\right)\left(-\frac{dZ}{dt}\right)_{max} T_{LVET} \tag{2.2}$$

This equation has limitations due to thorax being assumed as a cylinder, difficulty in determining the resistivity of the blood, and errors in the measurement of the effective length *L* [7]. An alternative equation has been proposed in which thorax is modeled as a truncated cone. In this equation, the resistivity of the blood is replaced by a value dependent on Z_0 (base impedance), *L* (length between the measuring electrodes), and volume. The volume is estimated as $L^3/4.25$ and *L* was found to be equal to 17 percent of a person's height *H* [7]. This equation is,

$$\Delta V = \left(\frac{(0.17\,H)^3}{4.25\,Z_0}\right)\left(-\frac{dZ}{dt}\right)_{max} T_{LVET} \tag{2.3}$$

This equation gives an error if a person's morphological makeup differs from the ideal body make-up. Bernstein [7] proposed a correction factor δ to scale the equation for deviation from ideal body weight**.** This equation is known as Sramek–Bernstein equation and uses both height and weight to estimate the electrode distance *L*, and the thoracic area instead of using the actual electrode distance *L*. It is given as,

$$\Delta V = \delta\left(\frac{(0.17\,H)^3}{4.25\,Z_0}\right)\left(-\frac{dZ}{dt}\right)_{max} T_{LVET} \tag{2.4}$$

By using this equation, morphological make-up of an individual can be accounted which eliminates the need to estimate the resistivity of the blood, and a decreased effect of basal impedance Z_0.

2.3 Electrodes

Type and placement of the electrodes, used for injecting the alternating current into the thorax and sensing the voltage developed across it, is important. Current injecting electrodes should be placed to ensure a nearly uniform current density in the thorax and voltage sensing electrodes should be placed such that the impedance variation due to blood flow in the aorta is maximum and the impedance variation due to the pulmonary circulation as well as blood ejection contracted by heart is very small. Two of the current injecting electrodes are placed across the thorax with one electrode placed at the root or base of the neck and another one is placed at the thorax around the xiphoid level. There are two types of electrode configurations frequently used in impedance cardiography, two-electrode and four-electrode or tetra-polar configuration. In the two-electrode configuration, injection of the current and voltage sensing is done by using the same pair of electrodes, In the tetra-polar configuration, two separate pairs of electrodes are used for current injection and voltage sensing. In the first configuration errors may introduced in the sensed voltage due to change in the contact impedance of the electrodes [3]. In the tetra-polar electrode configuration, the voltage sensing electrodes are placed between the current injecting electrodes near the thorax. In this method measured voltage is not affected by the contact impedance of the electrodes because a high input impedance amplifier is used for voltage sensing [3]. To estimate the stroke volume accurately, it is desired that the current density in the region between the electrodes should be uniform, thus voltage sensing electrodes should be placed such that the region between them should have approximately uniform current density distribution. Spot and band electrodes are two types of electrodes which are commonly used. Spot electrodes are easy to place on the thorax but they result in somewhat non-uniform current density [3]. Band electrodes provide more uniform current density but they are difficult to apply in clinical settings. They are also uncomfortable to wear and expensive. They cannot be used in long-term monitoring or ambulatory measurement [4], [7].

2.4 Impedance cardiograph hardware

The main hardware blocks of an impedance cardiograph include a current source, two electrode pairs for current injection and voltage sensing, impedance detector, differentiator, and an ECG amplifier [4], [9]–[15] as shown in Figure 2.3. The current source injects a high frequency and low amplitude current into the thorax through the current-injecting electrodes. This results in an amplitude modulated voltage across the thorax due to variation in the thoracic impedance. The voltage developed across the thorax is sensed by the voltage-sensing electrodes and is given to the impedance detector. The impedance detector consists of a high input impedance voltage-sensing amplifier, a demodulator and a baseline restoration circuit. The voltage-sensing amplifier amplifies the high frequency signal while rejecting artifacts and other noises. The demodulator extracts the impedance variation signal by amplitude demodulation. The baseline restoration removes the dc component for further amplification of the signal. The differentiator differentiates the pulsatile impedance signal and negative of the derivative is output as the ICG signal waveform. ECG extraction circuit extracts the ECG signal from the sensed voltage signal, and the extracted waveform is often used as a time reference for cardiac cycle in ICG processing.

2.4.1 Current source

It is advantageous to use current excitation as compared to voltage excitation as it minimizes the effect of electrode polarization and noise in the measurement caused due the impedance at skin-electrode interface. The current source should have high amplitude stability because any instability contributes to the noise in the sensed impedance signal. It should have high output impedance so that current injected in to the thorax is independent of the variation in the electrode-skin contact impedance. Its functioning should not get affected by common mode

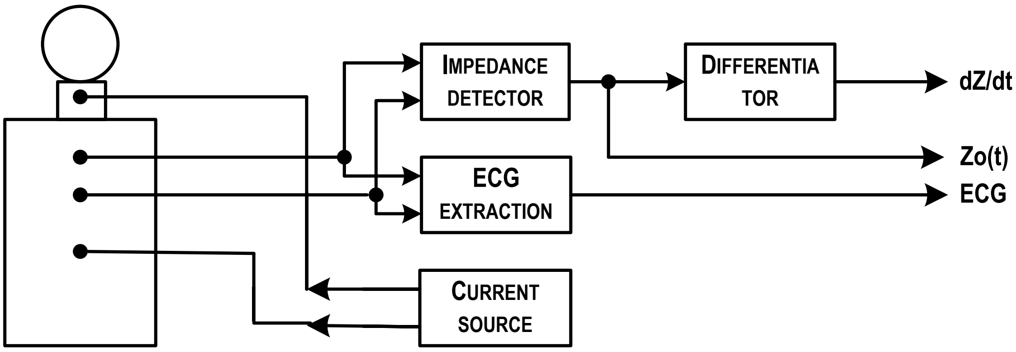

Figure 2.3 Block diagram of impedance cardiograph [14]

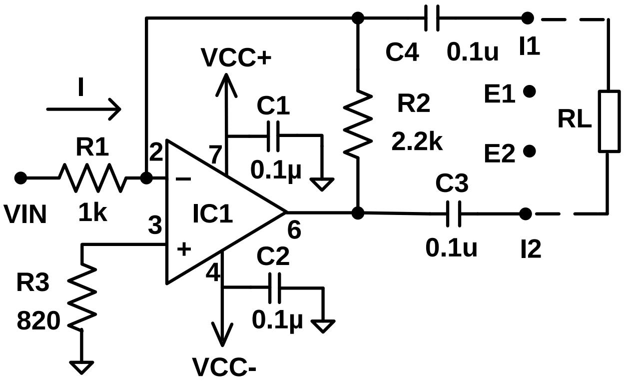

Figure 2.4 Circuit diagram of V-I converter with the load connected in feedback [13]. (IC1: LF356)

pick up, stray currents, and stray capacitances. Current source should be free of any dc to minimize errors due to the electrode polarization during measurement. Current source should be balanced in the sense that its two terminals should have nearly the same impedance with respect to the ground. It helps in reducing the effects of common mode pick-up, stray currents, and stray capacitance. Current source consist of a waveform generator or an oscillator and a V-to-I converter.

Several circuits have been reported to realize an oscillator [9]-[15]. Manigandan [9] and Naidu [10] used Wein-bridge oscillators. To improve the amplitude stability Venkatachalam [11] modified the Wein-bridge oscillator by introducing an amplitude stabilization loop using a peak detector and error amplifier. The frequency of a Wein-bridge oscillator cannot be varied easily. Use of voltage controlled oscillator (VCO) based circuits [16] permits a convenient control of the frequency. Sarvaiya et al [17] used a precision function generator IC and Patil [12] reported a circuit based on direct digital synthesizer (DDS) IC. The DDS based implementations provide excellent waveform stability [13].

The voltage signal is converted in to a current by means of a voltage- to current converter. An op-amp based inverting amplifier with the load connected in feedback can be considered as simplest design as shown in Figure 2.4. The output current is $I = V_{in} / R_1$.

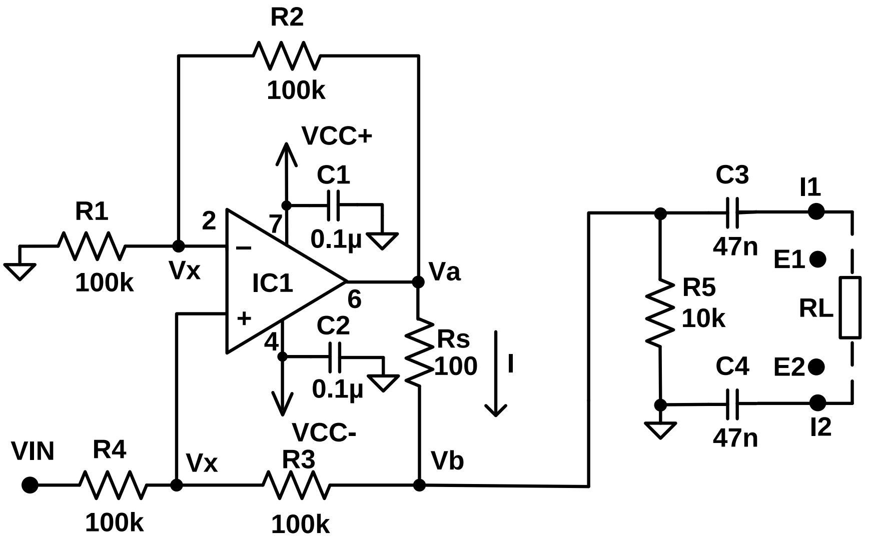

Figure 2.5 V-to-I convertor based on modified Howland current source [13]. (IC1: LF356)

Output is coupled through capacitors C3 and C4 to block DC current through the electrodes. In this design, one of the electrodes is at virtual ground and therefore two output terminals are not balanced with respect to the ground. Thus this circuit is sensitive to the stray currents and stray capacitances. A pulse transformer is used in [12] to get the balanced current outputs.

Modified Howland current source is used in [13] as shown in Figure 2.5. In this circuit, $I = V_{in} / R_s$. As none of the load terminals is connected to the virtual ground, instability due to stray capacitances at the op-amp input terminals is reduced. Resistance ratios R_2/R_1 and R_3/R_4 are needs to be matched in order to achieve high output impedance.

An enhanced Howland circuit and its simulation results are reported in [18]. This circuit consists of two similar current source circuits connected in parallel and same input signal is given to the input of both the op-amps and their outputs are connected to the load as shown in Figure 2.6. IC1 and IC2 are AD844 which is a high speed op-amp having slew rate of 2000 V/us. C8 and C9 used to block dc current flow. The output impedance of this circuit is approximately 100 kΩ as given in [18]. The output current is given as follows,

$$I_{out} = -V_{in}(1/R_3 + 1/R_7) \tag{2.5}$$

They have also considered the effect of the parasitic capacitors during simulation in the above circuit, parasitic capacitors deteriorate the performance of the source and circuit can become unstable, an inductor needs to be connected in parallel to the load to make this circuit stray insensitive. The inductor can be simulated by using op-amp and capacitor of any desired value as reported in [18]. Operational transconductance IC OPA861 from Texas Instruments is used to realize a balanced current source in [14] [15]. In the present design, as described later in chapter, the same design is used.

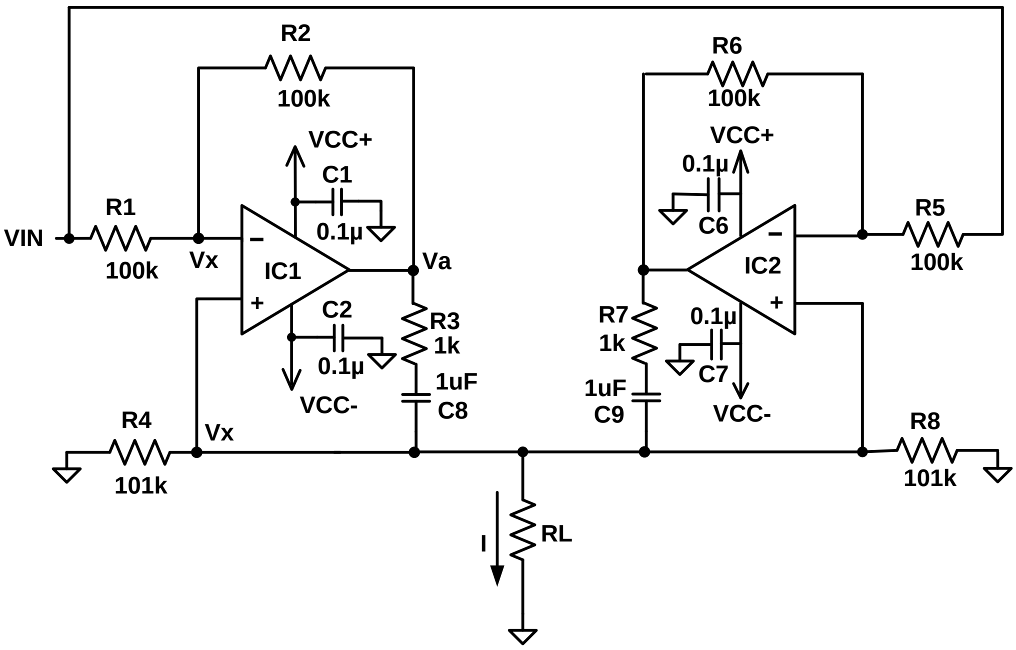

Figure 2.6 A Parallel enhanced Howland circuit [18]

2.4.2 Voltage sensing amplifier

The voltage sensed by the voltage-sensing electrodes is amplified by the voltage-sensing amplifier. This amplifier should have high input impedance, high CMRR, and a high pass response (> 10 kHz) so that it amplifies only the desired high frequency signal while rejecting the artifacts and other bio-potential signals [10] - [13]. An instrumentation amplifier IC is used as it provides very high CMRR over a wide frequency range.

2.4.3 Demodulator and baseline restoration

The sensed voltage after amplification must be demodulated to get the signal related to the impedance variation. The major challenge in demodulation is that the impedance of the thorax varies by a very small amount and hence the modulation index is very low (0.2 - 2%). Hence the demodulator should provide high sensitivity, carrier ripple rejection, and noise rejection. Most of the reported designs [9]-[12] have used precision full-wave rectifier based demodulation. Slicing amplifier based demodulator was used by Patil [10] for increasing the sensitivity. Synchronous sample-and-hold with sampling at carrier peaks was used for carrier ripple rejection. Synchronous demodulation scheme was used by Mishra [13], and Desai [14], this scheme is based on the current steering of the input through a reference current waveform which is in phase with the input signal of the demodulator. Figure 2.7 shows this synchronous demodulation scheme. Those components of the input signal which are in phase with the reference contribute to the output while the others which are not synchronous to or phase quadrature with the reference get rejected by low pass filtering. Hence noise and dc offset in the input get rejected. The reference square wave steers the input signals either to the ground

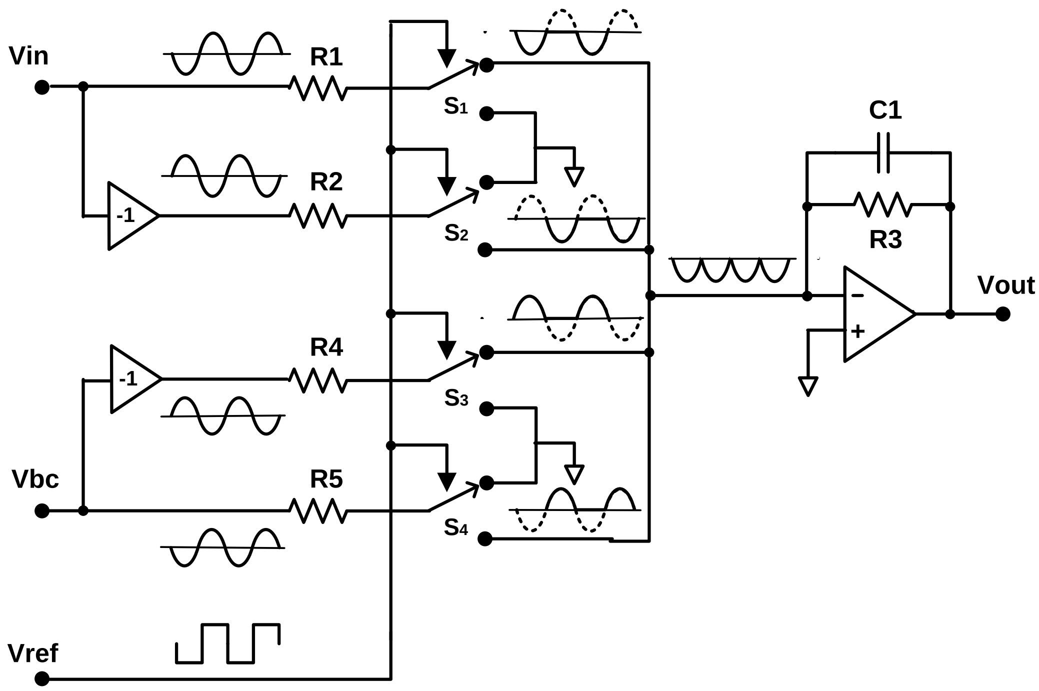

Figure 2.7 Demodulation using synchronous current steering with baseline correction [14]

or to the inverting terminal of the op-amp. A second sinusoidal current of opposite polarity is used for baseline correction. Rectified and baseline corrected signal then passed to the low pass filter that will give the impedance signal. In addition to the synchronous demodulation, this scheme provides the baseline correction by using switches S_3 and S_4, which removes the need to use extra hardware for the baseline correction.

2.5 Proposed design

In order to reduce overall chip count and for using digital synchronous demodulation, “Analog Devices AD5933” is used in the present design. The chip has a DDS core to synthesize the frequency and a 1024-point DFT processor. It has better noise rejection ability than earlier reported designs. A sinusoidal voltage obtained from the excitation source can be subtracted from the sensed voltage signal to increase its modulation index. This helps in increasing the dynamic range of the demodulator and also serves as a baseline correction by the amplitude of the voltage being subtracted. The proposed design will avoid most of the problems associated with the earlier circuits.

The impedance converter chip is not designed for measuring very small variations superimposed on a baseline impedance, but we have designed an analog front end to use it in our application. The analog front end consists of a current source, excitation and baseline amplitude control circuitry, and a baseline correction circuit to increase the modulation index before synchronous digital demodulation.

Chapter 3
THORACIC IMPEDANCE SIMULATOR

3.1 Introduction

A thoracic impedance simulator is needed for testing the linearity, sensitivity, and the dynamic response of the impedance measuring instrument. The time varying part of the simulated bio-impedance can be sinusoidal, triangular or a square wave. The square wave is simpler to generate and it can be used to find the dynamic response of the instrument and can be used for getting the frequency response. Hence, a square wave variation in resistance with a settable frequency and resistance is used in [19] The simulator has two terminal pairs, one pair each for connecting the current injecting and voltage sensing electrodes.

Various circuits have been reported earlier to implement the impedance simulator. The simulator has been redesigned [14] [15] to increase the number of basal resistance values in the range of 10 – 160 Ω. Thus, the simulator can be used for other applications involving bio-impedance measurement.

The simulator developed by Desai [14] and Bhat [15] can be programmed digitally by means of a microcontroller. This simulator provides 12 different values of the base resistance, but only a limited number of changes. The software of the microcontroller has been modified to get all changes from 0.1 Ω to 1 Ω, with a step of 0.1 Ω in resistance for each of the 12 values of the base resistance. A graphical user interface (GUI) has been developed in Visual Basic to control the circuit through PC. This modified impedance simulator has been tested for satisfactory results.

3.2 Bio-impedance model and impedance simulator realization

A bio-impedance model is shown in Figure 3.1 [19]. Time-varying bio-impedances sensed using two-electrodes, can be modeled as a time-varying resistive network. Resistance R_o represents the fixed resistance while resistance R_v represents impedance variation due to change in physiological activities. Electrode contact points are represented by E1 and E2. Resistances R_{E1} and R_{E2} represent the tissue-electrode contact impedance. The pickup voltage V_p in series with the resistance R_p is connected between the reference point A_{ref} and the ground of the impedance detecting instrument. Vp represents the common mode interference generated due to external pick-up and internal bio-electric signals while R_p represents the resistance of the common mode path.

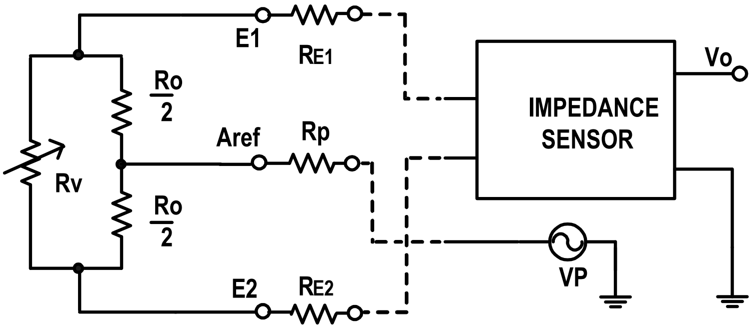

Figure 3.1 A model of impedance simulator [19]

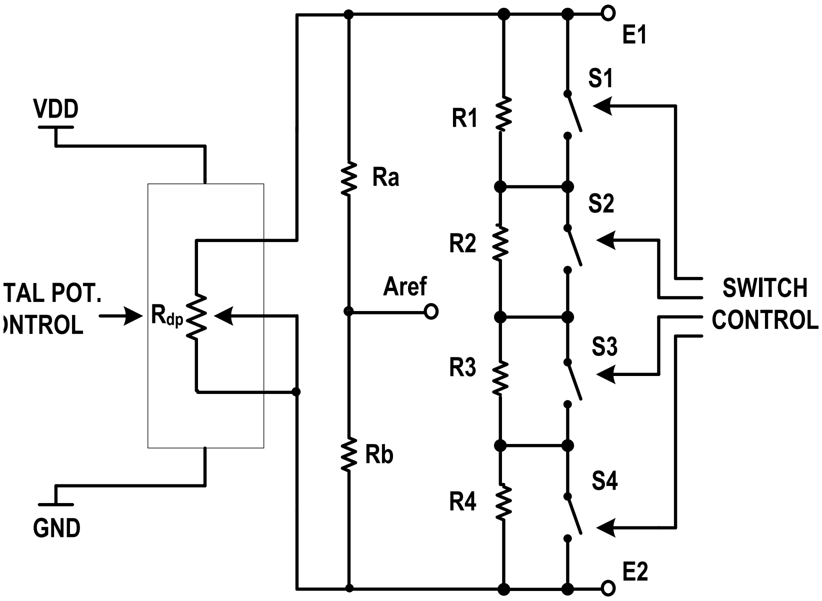

Figure 3.2 Schematic of bio-impedance simulator [14]

The total resistance across E1 and E2 is given by,

$$R_{E1E2} = R_0 || R_v \tag{3.1}$$

Variation in the resistance is implemented by using a digital potentiometer over a frequency of 0.1-1000 Hz. The wiper resistance of the potentiometer used is 50 Ω. therefore the digital potentiometer alone cannot be used to get the low basal resistance values. Therefore, a combination of resistors and analog switches having on-resistance less than 0.5 Ω are used. The schematic diagram of bioimpedance simulator is shown in Figure 3.2. Different combination of switches S1-S4 used to set different basal resistances. Digital potentiometer is used to achieve change in resistance. The equivalent resistance across terminals E1 and E2 is given by,

$$R_{E1E2} = R_{sw} || R_{dp} || (R_a || R_b) \tag{3.2}$$

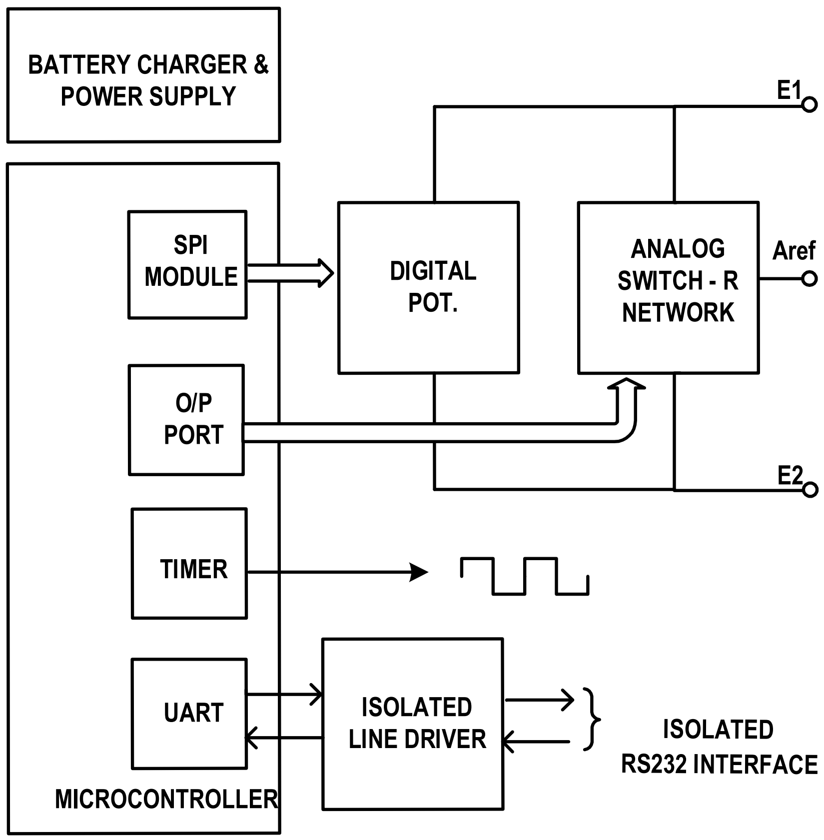

Figure 3.3 Block diagram of impedance simulator [14]

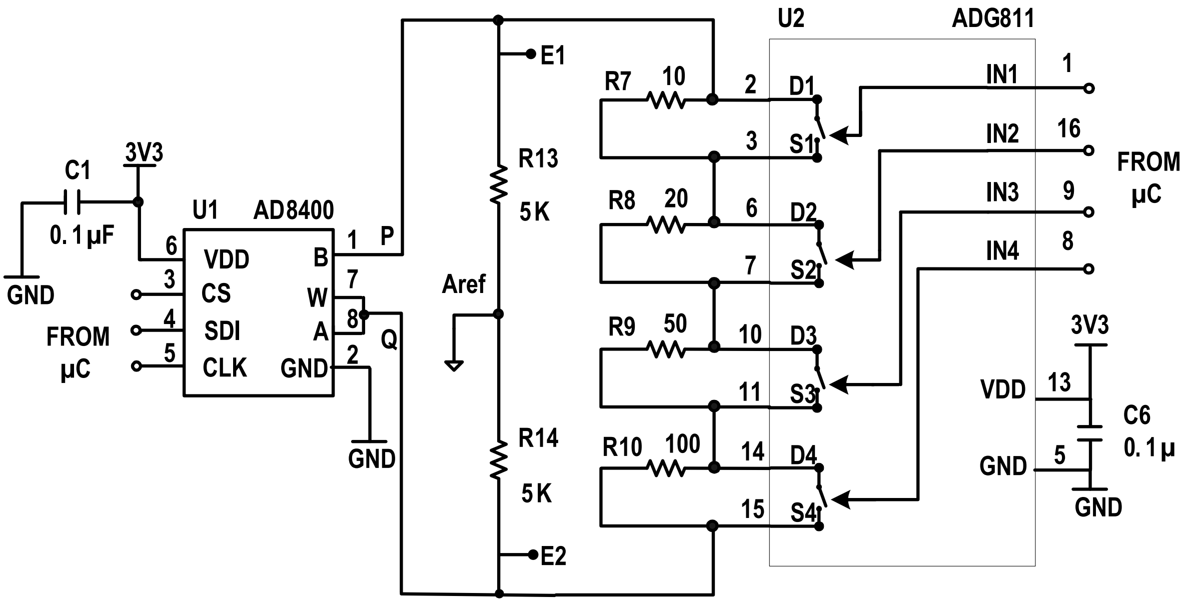

Figure 3.4 Resistance variation circuit [14]

Where, R_{sw} is the resistance obtained by control of combination of the resistors R_1,R_2,R_3 and R_4 through the analog switches and R_{dp} is the resistance of the digital potentiometer that can be controlled digitally through a microcontroller. Figure 3.3 shows the basic blocks of the impedance simulator. It shows the control from the microcontroller of digital potentiometer and isolated serial interface. On-chip timer of the microcontroller is used to generate the square wave with the set frequency. The interface is electrically isolated using "Analog Devices ADM3251E" for avoiding the possibility of coupling of the noise from the PC side.

The digital potentiometer "Analog Devices AD8400" [20] is used as U1. It has a resistance of 1 kΩ which can be varied in 256 steps from 0 Ω to 1 kΩ. The circuit is shown in Figure 3.4. It has a wiper resistance of approximately 50 Ω. Each step change of digital potentiometer changes its resistance by 4 Ω. This change in resistance in parallel with the basal resistance is used to get an overall resistance change of about 0.1 Ω. The digital potentiometer operates at 3.3 V with a maximum supply current of 1 mA. Quad analog switch "Analog Devices ADG811" [21] is used as U2. Its switches have on resistance less than 0.5 Ω the control voltage levels are compatible with the output port of the microcontroller. It operates at 3.3 V with a maximum supply current of 0.5 mA. We have used R7 of 10 Ω, R8 of 22 Ω, R9 of 56 Ω, and R10 of 120 Ω. These resistors along with the four analog switches can provide 12 settable resistances R_{sw} with nominal values of 10, 20, 30, 50, 60, 70, 100, 110, 120, 130, 150, and 160, by different combinations of switches as given in Table 3.1.The circuit formed by the switches and resistors is connected in parallel with the variable resistance R_{dp}. The resistance across E1 and E2 is given by,

$$R_{E1E2} = R_{sw0} || R_{dp} || (R_a || R_b) \tag{3.3}$$

where,

$$R_{sw} = S_1 R_7 + S_2 R_8 + S_3 R_9 + S_4 R_{10} \tag{3.4}$$

The value of S_1, S_2, S_3, and S_4 is 0 if the corresponding switch is closed or 1 if it is open. The resistance of the digital potentiometer is varied by digital control word transmitted to its serial register from the microcontroller. With S_1 and S_3 closed and S_2 and S_4 open, we get R_{sw} = 120 Ω, R_{E1E2} = 100 Ω for R_{dp} = 644 Ω. With R_{dp} changed to 636 Ω, we get R_{E1E2} = 99.9 Ω, i.e., ΔR = 0.1 Ω. [14].

The microcontroller "Microchip PIC24FJ64GB004" [22] is used for controlling the periodic change in the resistance at the set frequency, as shown in Figure 3.5. It has an in-built USB module, 4 programmable counters/timers, 2 SPI modules and 2 UART modules. The digital potentiometer is controlled using SPI module, analog switches via general purpose pins, and RS232 line driver is connected via UART module. The maximum operating clock frequency of the microcontroller is 32 MHz. Its internal RC oscillator with PLL is used for generating clock, thus eliminating the use of external clock or crystal. The microcontroller operates at 3.3 V, with a maximum current consumption of 16 mA. This interface is established using an isolated single channel RS232 line driver ADM3251E [23] as shown in Figure 3.5.

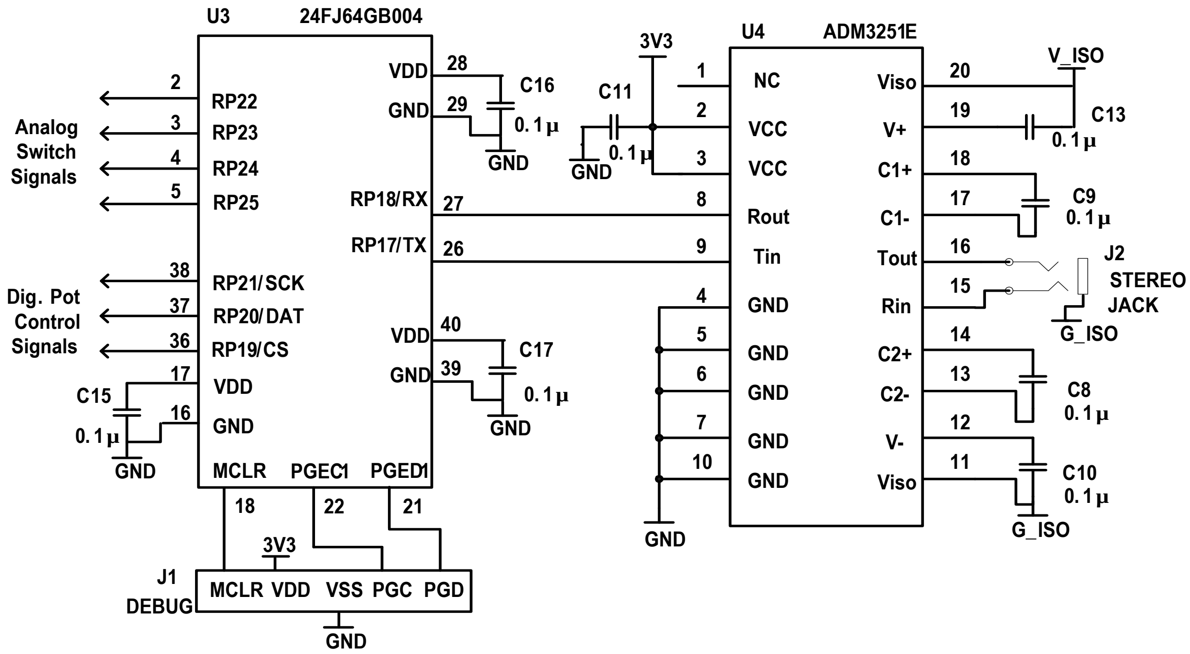

Figure 3.5 Microcontroller and serial line driver connections [14]

3.3 Software

The earlier microcontroller program [14] has been modified to get the change of 0.1, 0.2, 0.3.0.4, 0.5, 0.6, 0.7, 0.8, 0.9, and 1 Ω for each of the 12 values of the basal resistances. Program to control serial interface and to control the digital potentiometer has been written in embedded C. The algorithm can be described as following.

Main Program

1. Configure serial port for data transfer.
2. Set timer1 configuration bits to generate the required frequency.
3. Set the default values of digital potentiometer and analog switch.
4. Load timer registers with the counts according to the set frequency.
5. Set the simulation parameters when the serial interrupt occurs.

Interrupt Service Routine

I. If the interrupt is due to timer, do the following.

   1. Load the timer registers.
   2. Set digital potentiometer register by the specified value from the look-up table.
   3. Invert the SYNC pin to generate square wave on one of the pins of the microcontroller.
   4. Return.

II. If the interrupt is due to serial byte reception, do the following.

   1. Decode the received byte and set the different parameters.
   2. Update the analog switch controls.
   3. Return.

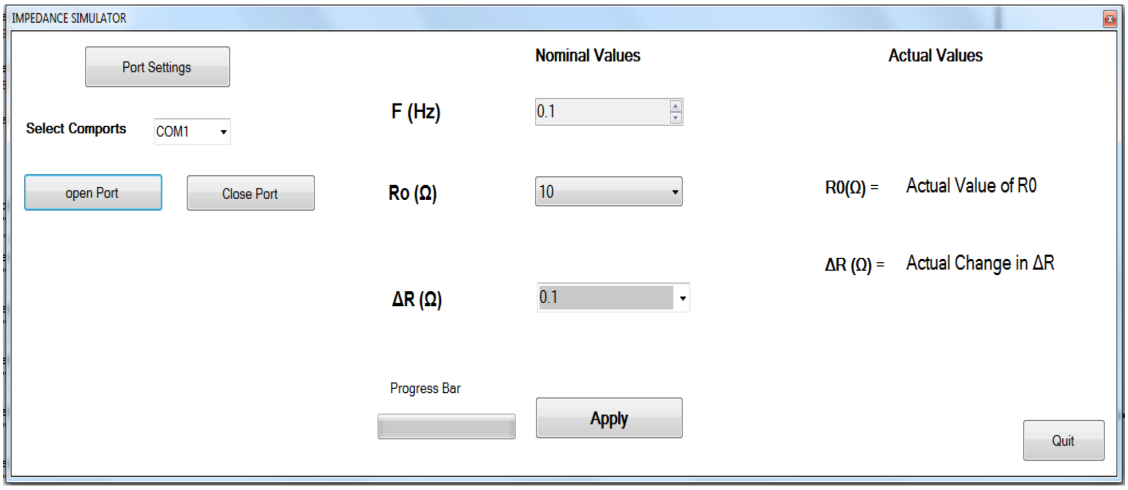

Figure 3.6 Screenshot of the user interface for impedance simulator

3.4 User Interface

A user interface has been developed for setting the parameters of the impedance simulator hardware implemented using Visual Basic. The frequency can be set from 0.1 Hz to 1 kHz. The base resistance can be selected from the dropdown list. A resistance change over the selected value of the base resistance can be selected from another dropdown list. Actual measured values of the base resistance and the corresponding change in it are shown against the desired values of the resistance. After press of “apply” button, selected values are sent via serial interface to the hardware. Figure 3.6 shows the screenshot of the user interface.

3.5 Test Results

Resistance values were measured using a digital multimeter (HP34401A) across terminals E1 and E2 for different combinations of switch positions (Figure 3.4) and resistance as set by the digital potentiometer. All values of change in resistance have been verified for each value of the base resistance. The calculated and corresponding measured values are given in Table 3.1 for a ΔR = 0.5 Ω. Table 3.1 shows the settings for the analog switches, digital potentiometers to get the desired base resistance, and the corresponding change in base resistance. Nominal values are the theoretical calculated values of the resistances and the measured values represent the actual resistance across the simulator terminals E1 – E2. The resistance value ΔR is the change when the digital potentiometer is changed from Rdp1 to Rdp2. The resistance across terminals E1-E2 with Rdp1 is taken as R and that with Rdp2 is taken as R-ΔR. The measured values show a good match with the nominal values. Periodic change in the resistance was also verified. For seeing the effect of

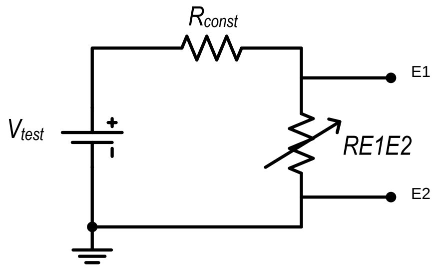

Figure 3.7 Impedance simulator as potential divider

switching at the resistance values across E1-E2, the voltage waveform in the time varying potential divider circuit of Figure 3.7 was observed. Examples for switching frequency of 0.3 Hz, 0.5 Hz, and 100 Hz are shown in Figure 3.8.

Table 3.1 Change in resistance 0.50 Ω (ΔR) for different values of base resistance R

Switch Status				**Digital pot. settings**		**Resistance across E1-E2**			
						Nominal		Measured	
S1	S2	S3	S4	R_{dp1}(Ω)	R_{dp2}(Ω)	R(Ω)	ΔR (Ω)	R(Ω)	ΔR (Ω)
1	0	0	0	206	86	10	0.5	9.8	0.52
0	1	0	0	136	112	20	0.5	19.8	0.50
1	1	0	0	948	589	30	0.5	29.6	0.55
0	0	1	0	331	303	50	0.5	49.8	0.55
1	0	1	0	643	577	60	0.5	59.7	0.49
0	1	1	0	635	589	70	0.5	69.7	0.52
0	0	0	1	522	507	100	0.5	99.6	0.50
1	0	0	1	706	679	110	0.5	109.6	0.55
0	1	0	1	761	737	120	0.5	119.5	0.53
0	1	1	1	874	854	160	0.5	159.5	0.53

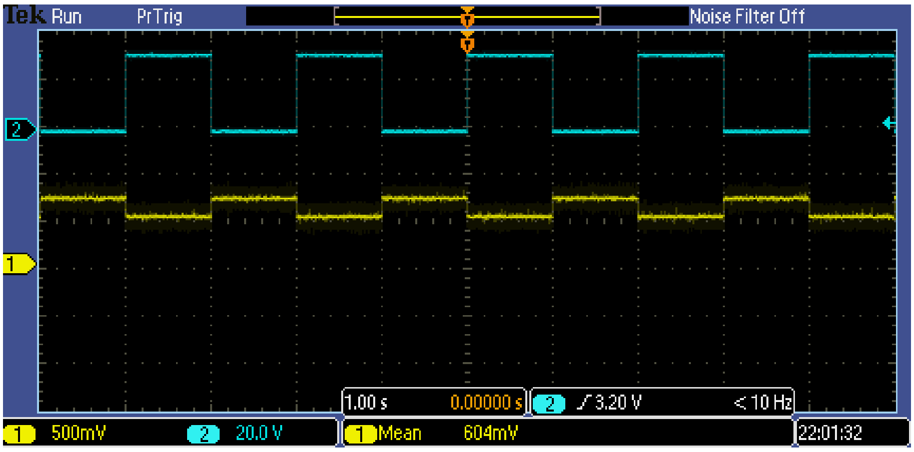

(a) F = 0.5 Hz

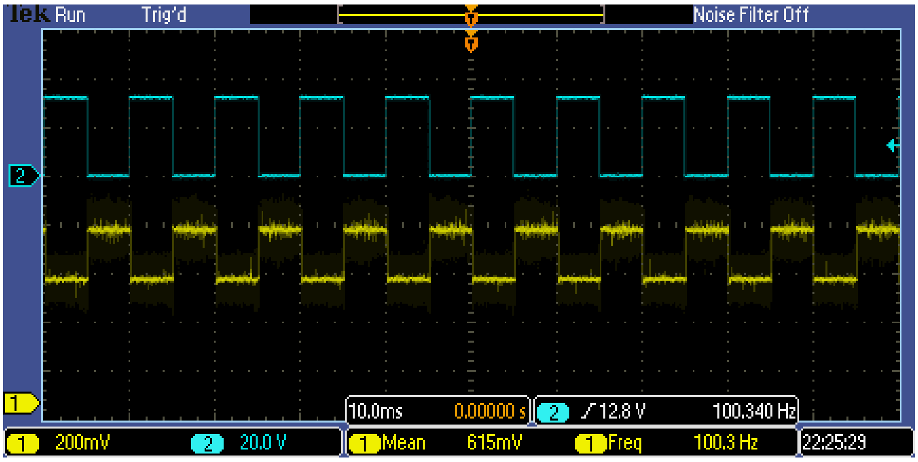

(b) F = 100 Hz

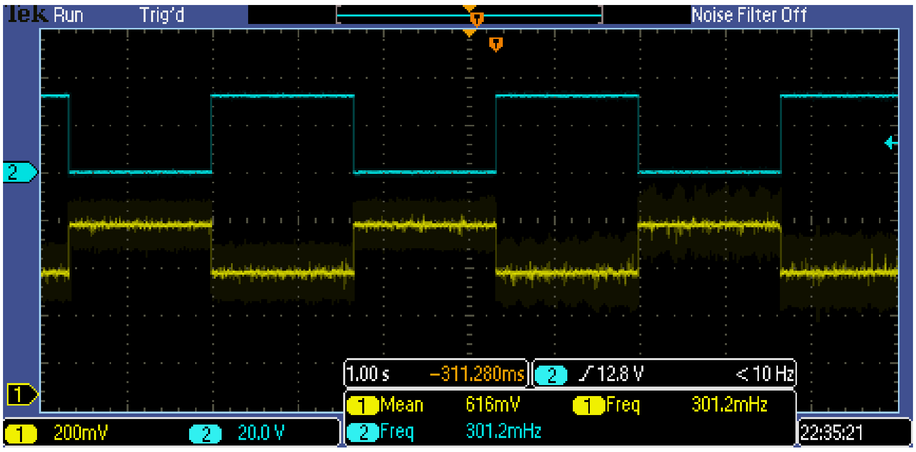

(c) F = 0.3 Hz

Figure 3.8 Output of time-varying potential divider in figure 3.7, with R = 100 Ω, ΔR = 50 Ω, channel 1: Output from port pin RB5, channel 2: Output across impedance simulator circuit.

Chapter 4

IMPEDANCE CARDIOGRAPH HARDWARE AND SOFTWARE

4.1 Overview

The main hardware blocks of an impedance cardiograph include a current source, two electrode pairs for current injection and voltage sensing, impedance detector, differentiator, and an ECG amplifier [4], [9]–[15]. The current source injects a high frequency and low amplitude current into the thorax through the current-injecting electrodes. This results in an amplitude modulated voltage across the thorax due to variation in the thoracic impedance. This amplitude modulated voltage is sensed using another pair of electrodes and amplified by the voltage-sensing amplifier. The amplifier should have high CMRR and it should amplify the desired high frequency signal while rejecting other bioelectric signals and noise. A high-pass filter with cut-off greater than 10 kHz can be used before the amplifier for this purpose. The demodulator demodulates the amplitude modulated voltage amplified by the voltage-sensing amplifier to extract the impedance variations. Since the thoracic impedance varies by 0.2 Ω, the modulation index is very low (0.2 - 1%). Hence the major challenge in the design of demodulator is its sensitivity so that it is able to detect the small amplitude variations. Also it should provide good noise rejection, carrier ripple rejection and low distortion. The ECG extraction circuit uses the same pair of electrodes as used for voltage sensing. The ECG obtained is used as a reference for processing the ICG signal and is generally not used for diagnostic purpose. The voltage developed across the thorax is sensed by the voltage-sensing electrodes and is given to the impedance detector. The impedance detector consists of a high input impedance voltage-sensing amplifier, a demodulator and a baseline correction circuit. The voltage-sensing amplifier amplifies the high frequency signal while rejecting artifacts and other noises. The demodulator extracts the impedance variation signal by amplitude demodulation. The baseline correction removes the DC component for further amplification of the signal, it improves the modulation index. The differentiator differentiates the pulsatile impedance signal and negative of the derivative is output as the ICG signal waveform. ECG extraction circuit extracts the ECG signal from the sensed voltage signal, and the extracted waveform is often used as a time reference for cardiac cycle in ICG processing.

Several circuits have been reported earlier [9] - [15] for implementing these blocks. In earlier designs, reported in [13], [14], and [15], a direct digital synthesizer (DDS) was used

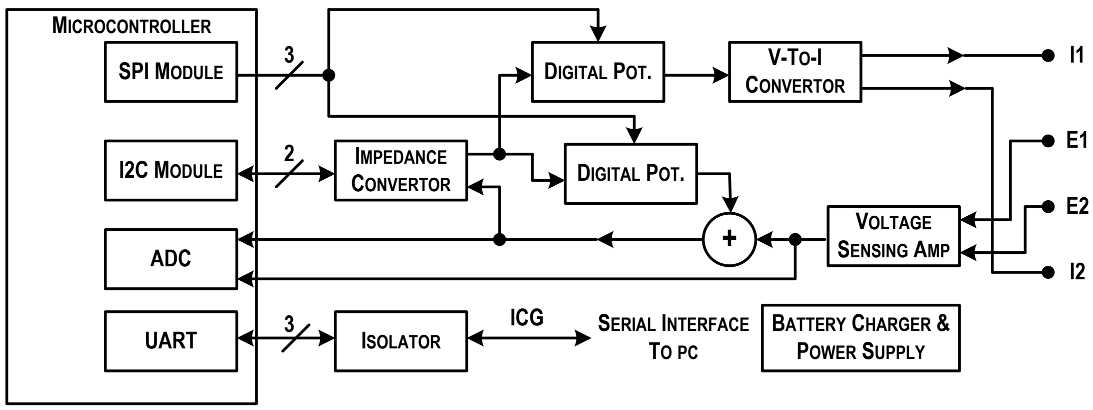

Figure 4.1 Block diagram of the impedance cardiograph circuit

for generating the sinusoidal excitation for high amplitude stability and settable frequency. Operational transconductance amplifier was used to realize voltage-to-current converter. Synchronous demodulator using current steering was implemented for high noise rejection, carrier ripple rejection and automatic baseline correction.

In order to reduce overall chip count, a new circuit based on an impedance converter IC “Analog Devices AD 5933”, is developed and tested. The chip has a DDS and a digital synchronous demodulator. As described in section 4.2, the chip uses voltage excitation for impedance measurement. For bioimpedance measurement, current excitation is preferred. Further we need to have a high sensitivity measurement with baseline correction. We also need to ensure that no DC current gets injected into the thorax in order to prevent the electrode polarization at the measuring electrodes. Another challenge is that impedance cardiography involves measuring a small time varying component of the impedance. Hence we need to devise a circuit for dynamic baseline correction and settable sensitivity without sacrificing the advantage of digital synchronous demodulation. Hence for using AD5933 in impedance cardiography, we need to devise appropriate external hardware. A new circuit for the impedance cardiograph using this IC has been conceptualized, designed and tested based on the digital synchronous demodulation using the Impedance converter IC AD5933.

Figure 4.1 shows the block diagram of the circuit. A microcontroller is used for setting all the measurement parameters, data transfer using serial data transfer, and for dynamic baseline correction with settable sensitivity. The output voltage signal from impedance converter is given to a V-to-I converter. The converter generates a balanced current output which is injected into the thorax using the electrode pair I1–I2. The voltage generated across the thorax is sensed using another electrode E1–E2. This sensed voltage is fed to an instrumentation amplifier. A baseline correction is realized using a summer amplifier. Two digital potentiometers are used for independent control of the excitation current and baseline correction. The output of the baseline correction circuit is given as input to the demodulator of the impedance converter. The output of the sensing amplifier and the summer for baseline correction are applied to two ADC inputs of the microcontroller and the values are used for setting the configurations of the digital potentiometers for the excitation current and baseline correction, respectively. The measured digital output is sent to the PC over the RS232 serial interface.

4.2 Impedance converter AD5933

AD5933 is a high precision impedance converter chip [24]. It consists of a direct digital synthesizer for stable sinusoidal signal generation, an op-amp for current-to-voltage converter, a low pass filter, a 12-bit ADC and a DFT based synchronous demodulator which gives real and imaginary part of the impedance. The synchronous demodulation feature is very important for rejecting noise. The basic circuit configuration for using the impedance converter for impedance measurement as given in the datasheet is shown in Figure 4.2. The chip has been designed for measuring impedance with almost no external component by providing voltage output across unknown impedance and sensing the resulting current flowing through it using on-chip current-to-voltage converter.

It has separate analog and digital power supplies of 2.7 – 5.5 V with maximum supply current of 15 mA at 3.3 V. This chip can be clocked either by on-chip RC oscillator or using an external oscillator [24]. In our application, it is clocked by on-chip oscillator of 16.77 MHz. It has I2C serial interface (SCL, SDA) which is used for programming the operation of the chip and for reading the measured values. In our design, the impedance converter U1 (AD5933) is interfaced with the microcontroller U8 (PIC24FJ64GB004), via I2C serial interface as shown in Figure 4.3. The clock SCL and data SDA pins of the chip are connected to the microcontroller pins RP2 and RP3 respectively. The SDA and SCL pins used for I2C serial communication are open drain pins and therefore pull-up resistors R_{18} and R_{19} of 10 kΩ are provided. I2C data rate can be set to 100 kHz or 400 kHz. The DDS of AD5933 can generate frequency up to 100 kHz with a resolution of 0.1 Hz. The frequency can be swept in accordance with the set parameters. In our application the synthesizer is to be operated at a fixed frequency with 40 - 100 kHz range. The frequency is programmed via a 24-bit word loaded serially over the I2C serial interface to the frequency increment register [24].

The DDS output frequency f_{out} can be calculated as,

$$f_{out} = (N_{freq} / 2^{27}) (MCLK / 4) \tag{4.1}$$

where N_{freq} is the value written in the start frequency register, and MCLK is the clock frequency. The peak-to-peak value of the output sinusoidal excitation signal can be programmed with a maximum value of up to 2V [24]

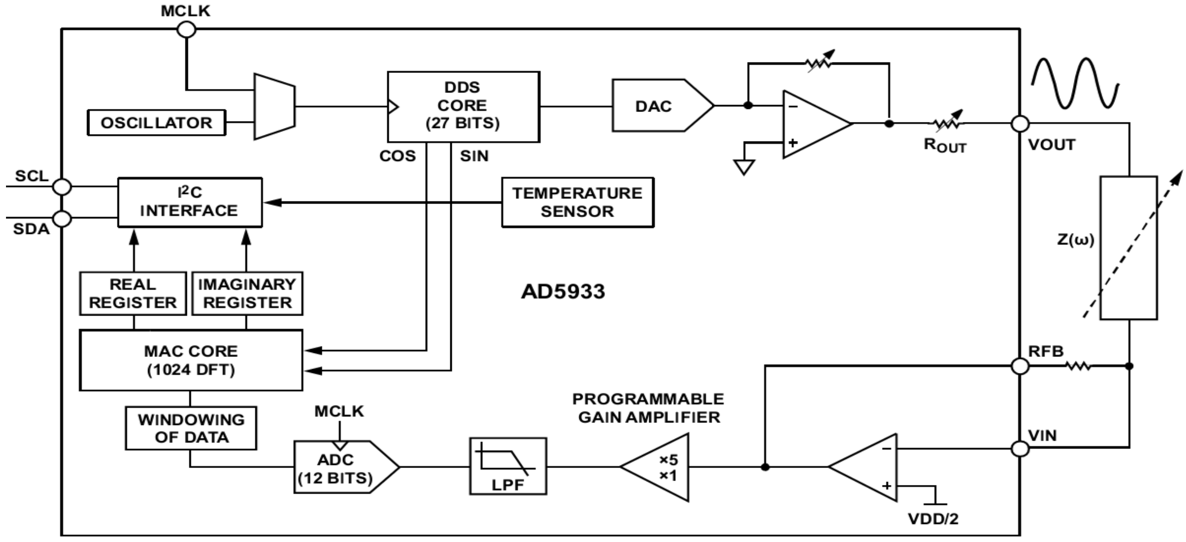

Figure 4.2 Functional bloack diagram of impedance convertor AD5933 [24]

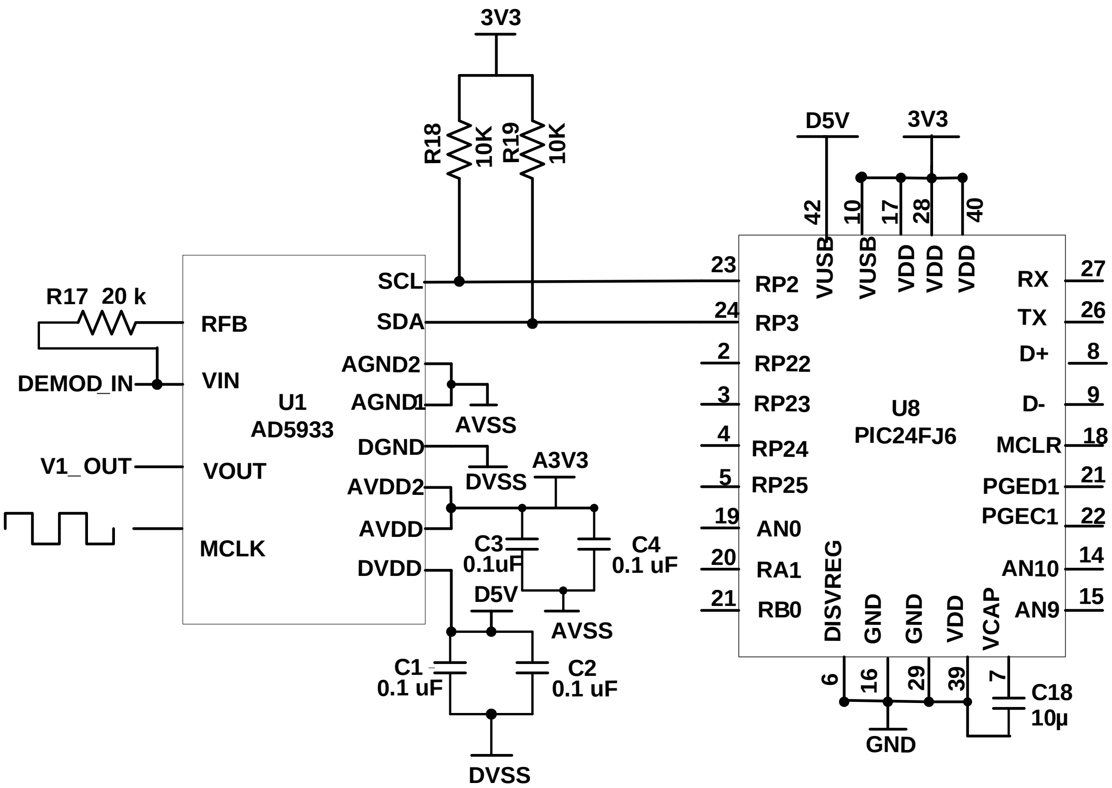

Figure 4.3 Impedance convertor and microcontroller [U8: PIC24FJ64GB004] connections

The synthesized voltage output is applied to one end of the unknown impedance *Z(ω)*, while its second end is connected to VIN terminal of the internal op-amp, which is virtually at $V_{DD}/2$. With resistor R_{FB}, on-chip op-amp acts as a current-to-voltage converter.

The op-amp output V_{sense} results in

$$V_{sense} = V_{DD}/2 \; - R_{FB}\,(V_{out} - V_{DD}/2\,)/Z(\omega) \qquad (4.2)$$

This sensed voltage after amplification and low-pass filtering is sampled by on-chip ADC. For measuring the complex impedance digital synchronous demodulation is carried out by calculating a 1024-point DFT of the sampled values *x*(*n*), at the excitation frequency *f*, using,

$$X\,(f) = \sum_{n=0}^{1023} x(n)\,\exp^{-j2\pi n \frac{f}{f_s}} \qquad (4.3)$$

where f_s is the sapling frequency. For this chip, the sampling frequency is specified to be of 1.04 MHz with the master clock of 16.77 MHz from the internal RC oscillator. The result is stored in two 16-bit registers representing the real part X_R and X_I the imaginary components of the result. The data are stored in two's complement format. The values can be transferred to a microcontroller over I2C serial interface for calculating the impedance.

Magnitude and phase of the measured value can be calculated as,

$$|X| = \left({X_R}^2 + {X_I}^2\right)^{0.5} \qquad (4.4)$$

$$ø_{\mathrm{X}} = \tan^{-1}(X_I/X_R) \qquad (4.5)$$

This magnitude $|X|$ is proportional to the current through the unknown impedance and hence it is inversely proportional to the unknown impedance. The calibration factor is obtained by calibrating the measuring system by connecting a known resistance R_C and recording the corresponding measured magnitude as $|X_C|$ This is used for obtaining the unknown impedance *Z* from the measured values $|X|$ and $ø_X$ as following,

$$|Z| = R_c X_c/|\mathrm{X}| \qquad (4.6)$$

$$ø_{\mathrm{Z}} = -\,ø_{\mathrm{X}} \qquad (4.7)$$

4.3 Bioimpedance measurement using AD5933

The design uses a microcontroller for controlling the operation of the various circuit blocks and reading X_R and X_I from the impedance converter chip. Microcontroller chip "Microchip PIC24FJ64GB004" is used as U8 along with the impedance converter as U1 as shown in Figure 4.3. The circuit given earlier in Figure 4.2 uses voltage excitation and hence it is not suitable for bioimpedance measurement, where current excitation is preferred. Thus a separate analog front-end is designed which includes circuits for amplitude-controlled voltage-to-current converter, voltage sensing amplifier, and controlled-baseline correction circuits.

In our application, current excitation is used thus the magnitude $|X|$ is proportional to the voltage across the unknown impedance and hence it is proportional to the unknown

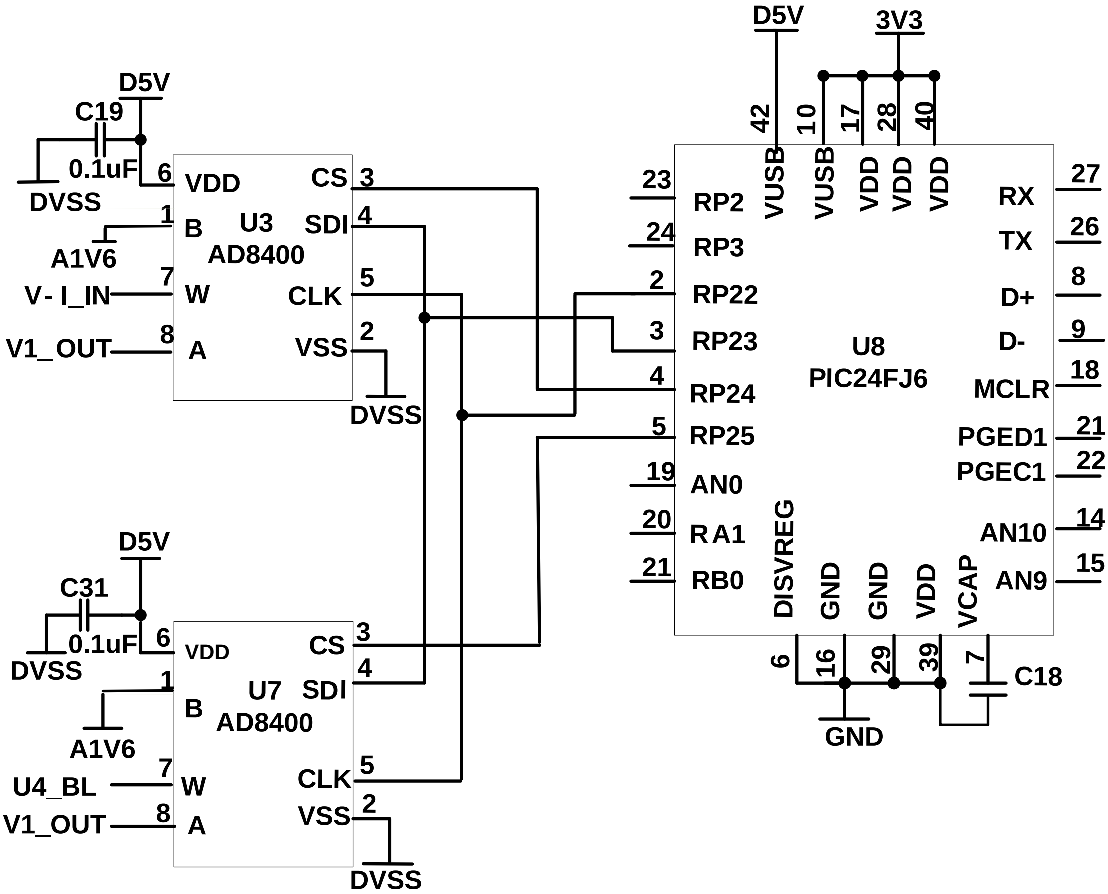

Figure 4.4 Amplitude control using digital potentiometers, AD8400

impedance and is calculated as,

$$|Z| = (R_c/X_c)|\mathrm{X}| \tag{4.8}$$

4.4 Current excitation with amplitude control

Waveform amplitude control is necessary for changing the amplitude of excitation current and baseline correction signal. The voltage from DDS of the impedance converter can only be programmed to be one of the four values with dc offset. An external digital potentiometer is used for flexibility in amplitude control. This output voltage V1_OUT (Figure 4.3) from U1 is fed as input to digital potentiometer U3, as shown in Figure 4.4. Its output is used as input V-I_IN (Figure 4.6) of the V-to-I circuit to control the amplitude of the excitation current. As shown in Figure 4.4, the amplitude control is realized using digital potentiometer "AD8400" as U3. It operates with single supply of 2.7-5.5 V with a supply current of 1 mA. It has a total resistance of 1 kΩ with 8-bit resolution and the wiper resistance of 50 Ω. [20]. The wiper position is controlled using SPI interface. The voltage input for baseline correction is independently controlled by using another digital potentiometer U7. Both the digital potentiometers are controlled by the microcontroller U8.

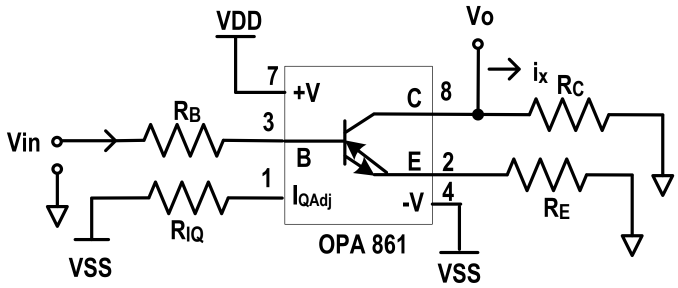

Figure 4.5 Basic circuit of A V-to-I convertor based on operational transconductance amplifier OPA861

The V-to-I converter converts the voltage output from digital potentiometer U3, to the current signal. Current source output impedance should be sufficiently high so that changes in the values of the tissue-electrode impedance and the thoracic impedance do not affect the current injected into the thorax. It should also be insensitive to common mode pickup and stray currents.

In the present design, V-to-I converter is realized using the operational transconductance amplifier (OTA) IC "TI OPA861" [25]. The basic circuit is shown in Figure 4.5. OTA can be considered as a super transistor, with the C-output current flowing out the C terminal for positive B-to-E voltage and into the C terminal for negative B-to-E voltage. Its emitter can source as well as sink current. It can be operated with a single supply of +5 V as well as dual supply of ± 5 V. It has a bandwidth of 80 MHz, and slew rate of 900 V/µs. The transconductance is 90 mA/V at quiescent current of 4.7 mA with +5 V supply voltage. Transconductance is a function of the quiescent current which is set with a resistor R_{IQ}, connected from pin 1 to ground. The transconductance is constant over a wide range of collector currents. The output current is given as,

$$i_x = V_{in}/(R_E + 1/g_m) \tag{4.9}$$

where, g_m is trans-conductance and R_E is the emitter resistance Thus the output current is proportional to the input voltage and can be controlled by varying R_E.

In the present design, a balanced current source is implemented using two OTAs. The circuit is shown in Figure 4.6. The OTA's are powered by a single +5 V supply with the reference terminal A1V6 at 1.65 V with reference to V_{SS}. The reference voltage is the same as used in other parts of the circuit. The currents Iout1 and Iout2 are given as,

$$I_{out1} = (\beta V_{in} - V_{ref})/(R_2 + 1/g_{m1} + 1/g_{m2}) \tag{4.10}$$

$$I_{out2} = I_{out1} \tag{4.11}$$

Where g_{m1} and g_{m2} are the transconductances of U4 and U5 respectively, and β is the digital potentiometer (U3) ratio which is used to attenuate the input voltage in order to

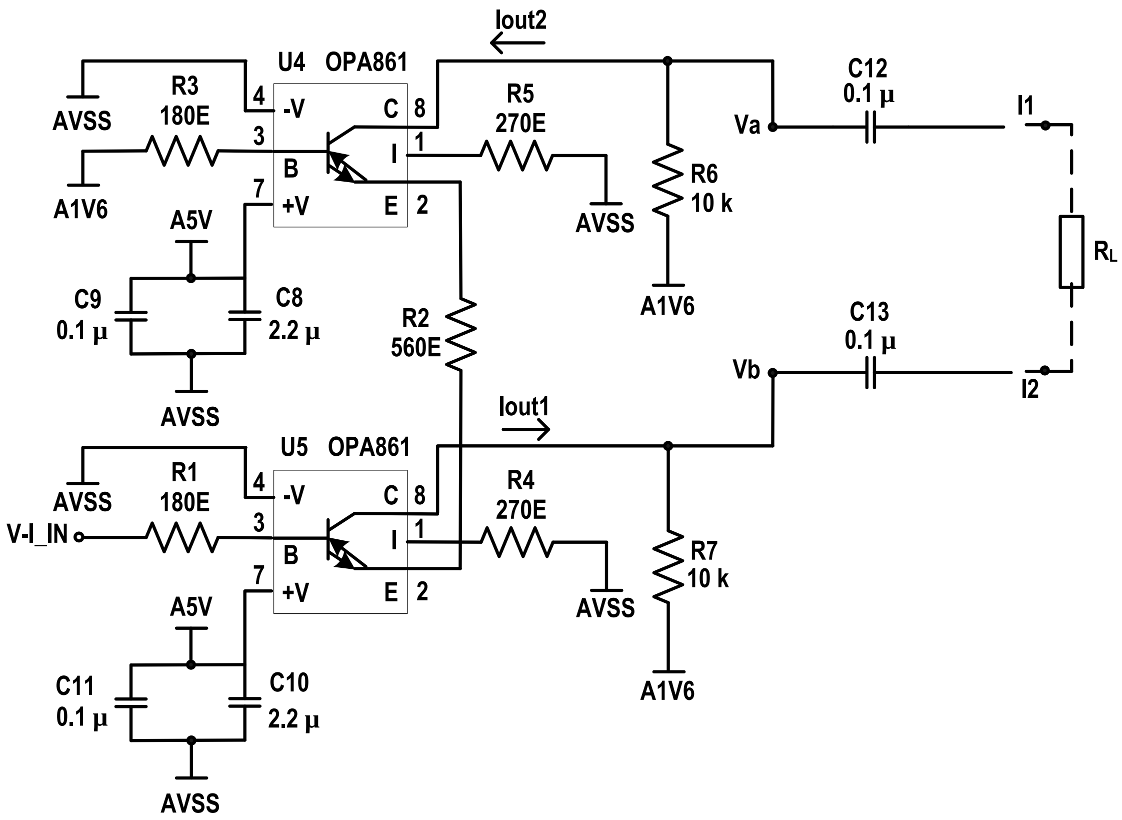

Figure 4.6 V-to-I convertor realized using operational transconductance amplifier

vary the input excitation current. V_{in} is the input V-I_IN (Figure 4.6) voltage and V_{ref} is the dc reference voltage of 1.65 V.

The circuit eliminates the need of a transformer to get balanced current outputs. The voltage V_{in} is set at 1.5$V_{p\text{-}p}$. With emitter resistance R_2 560 Ω and assuming β to be unity, the maximum current output is confined to ± 2.5 mA. As the transconductance g_m is 90 mA/V, we get 1/ g_m 11.1 Ω. The circuit can go into saturation due to the improper tissue electrode contacts or if impedances between the two output terminals and the voltage reference terminal are unbalanced. Resistors R6 and R7 to prevent saturation of output voltage, but they limits the output resistance of each terminal of the current source to 10 k Ω. Capacitors C12 and C13 are used to block the dc current passing through the electrodes. The impedance offered by these capacitors at the excitation frequency should be very small compared to unknown impedance. C12 = C13 = 0.1 uF at f = 50 kHz corresponding to an impedance of 3.18 Ω. This output current is injected into the thorax by current injecting electrodes I1 and I2.

4.5 Voltage sensing amplifier

An instrumentation amplifier is used to sense and amplify the voltage across the thorax using the separate electrode pair E1-E2. The desired characteristics of voltage sensing circuit are

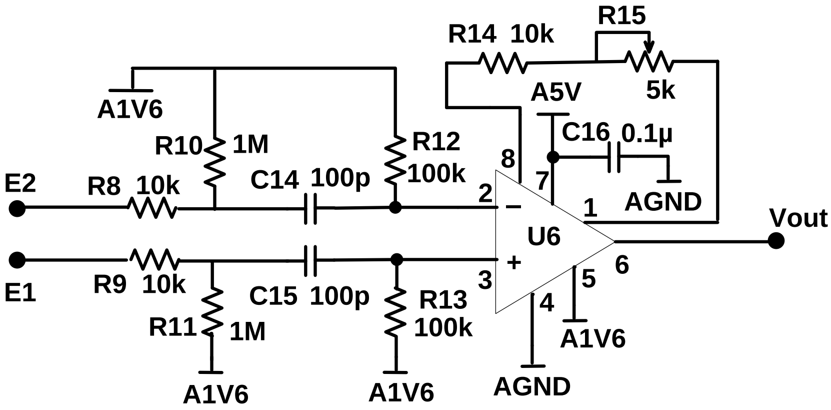

Figure 4.7 Voltage sensing Amplifier (U6: INA155)

high input impedance, high CMRR. Figure 4.7 shows the circuit of voltage sensing amplifier, where U6 is an instrumentation amplifier "TI INA155" [26] from Texas instruments, as used earlier in [13]. This has high CMRR of 100 dB at 100 Hz and a slew rate of 6.5 V/µs. It offers gain bandwidth product of 5.5 MHz. it works with a single supply 2.7- 5.5 V and provides rail-to-rail output swing. The gain of the amplifier can be set by a resister connected between pin 1 and 8. In our design, a variable resistor of 5 kΩ is connected in series with a fixed resistance of 10 kΩ to get a variable gain in the range of 10-35 at excitation frequency. Gain of amplifier can be calculated by the following formula,

$$G = 10 + \left(\frac{400k\Omega}{10k\Omega + R_G} \right). \qquad (4.12)$$

Where R_G is the external resistance connected between the pins 1 and 8. The two inputs are RC coupled through a first order high-pass filter to reject noise and other bio-electric signals, whose cutoff frequency is given as,

$$f = 1/2\pi RC \qquad (4.13)$$

Where R_{12} = R_{13} = R and C_{14}= C_{15} = C. We use R = 100 kΩ and C = 100 pF, for f = 16 kHz. This helps in rejecting artifacts and noise voltages without affecting the sensed voltage. Resistors R8 and R9 are used for patient safety by limiting any accidental current through the electrodes. Resistors R10 and R11 are used to block any dc current path to the electrodes. This filtered output is given as an input to the instrumentation amplifier. The output of the voltage sensing amplifier is applied as one of the two inputs of baseline correction circuit.

4.6 Baseline correction circuit

Bio-electric signals are generally superimposed on a baseline. The baseline of the thoracic impedance signal can be easily affected by breathing, motion artifacts, and variation in skin resistance. This may cause the baseline wander. When this time varying shift in the baseline is large, the resulting output may saturate and the measured bioimpedance signal may be erroneous. Although baseline drift can be cancelled, using digital signal processing techniques these can be applied only of the input signals are within the input range of the ADC to prevent the signal saturation. A dynamic correction of the baseline wander before analog- to digital conversion permits amplification of the signal and a more effective use of the input dynamic range of the data acquisition circuit. In our design, the synchronous digital demodulation takes place in the impedance converter chip and the demodulator's intermediate stage outputs are not accessible. Further the demodulation has an accuracy of 0.5% and hence it cannot be used for signals with modulation index of 0.2-1%. Therefore a baseline correction circuit is needed to increase the effective modulation index by subtracting a sinusoidal reference voltage from the sensed voltage before applying it as input to the demodulator.

As the polarity of the sensed voltage signal with reference to the excitation current may get inverted due to interchange of electrodes, we need a baseline correction circuit in which the amplitude and polarity of the correction voltage can be digitally controlled. The circuit schematic devised for this purpose is shown in Figure 4.8. Op-amp U18 is used as a summing amplifier, which adds signal voltage $V_{s.}$ and the correction voltage V_{bc}. With the help of digital potentiometer, the gain can be varied over ±1 for baseline correction signal V_{bc}. This output is sampled by ADC of the microcontroller and compared with the upper threshold voltage V_{ut} and lower threshold voltage V_{lt}. If the value is outside the specified thresholds, the digital potentiometer count needs to be modified in order to bring the output within the set threshold limits, so that the input to the demodulator does not saturate and the signal is not too low. The output of U18 in Fig.4.8 is given as

$$v_0 = A_s V_s + V_{bc}\,(A_{bc} + \alpha\, A_c) \tag{4.14}$$

where all the voltages are with refer to A1V6 and

$$A_s = -R_{35}/R_{34}$$

$$A_{bc} = -R_{35}/R_{33}$$

$$A_c = 1 + R_{35}/(R_{33}\,||R_{34})$$

$$V_s = [\beta V_{bc}\,/(R_E + 2/g_m)]ZG$$

The voltage V_{bc} is the output at V1_OUT of the DDS U1 in Figure 4.3. Voltage V_s is the output at Vout of U6 in Figure 4.7. The resistance ratio β is obtained from digital potentiometer U3, and is used to vary current excitation. The resistance ratio α is obtained from digital potentiometer U7 used to vary baseline correction signal. R_E and g_m are the current source parameters used to set the desired current amplitude. Z is the effective value of bioimpedance across the voltage sensing electrodes, G is the gain of the voltage sensing amplifier.

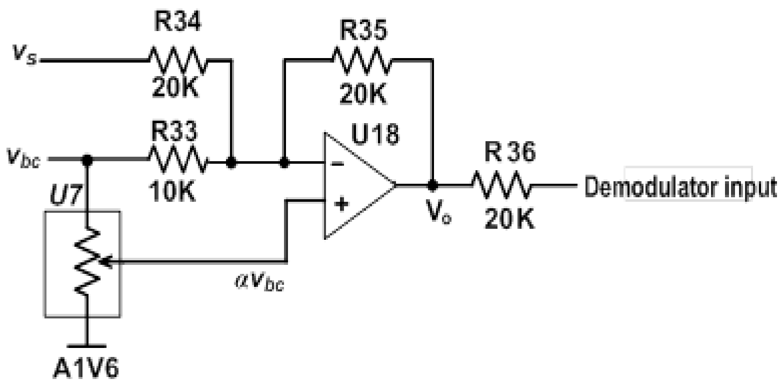

Figure 4.8 Schematic of summing amplifier for baseline correction (U18: AD8605 [27],U7: AD8400)

By selecting R_{33}/R_{34} = 0.5 and R_{35} = R_{34}, we get $A_s = -1, A_{bc} = 2,$ and $A_c = 4$. Therefore Eq. 4.14 becomes,

$$v_0 = V_{bc}\,[2(2\alpha - 1) - \beta ZG/(R_E + 2/g_m)] \tag{4.15}$$

Let, $K = \beta G/(R_E + 2/g_m)$. we get,

$$v_0 = -V_{bc}\,K(Z - 2(2\alpha - 1)/K) \tag{4.16}$$

This results in

$$v_0[\alpha = 0.25] = -V_{bc}\,K(Z + 1/K) \tag{4.17}$$

$$v_0[\alpha = 0.75] = -V_{bc}\,K(Z - 1/K) \tag{4.18}$$

$$v_0[\alpha = 0.5] = -V_{bc}\,K(Z) \tag{4.19}$$

$$v_0[\alpha = 0.5 + \Delta\alpha] = -V_{bc}\,K(Z - 4\Delta\alpha/K) \tag{4.20}$$

Thus the input voltage is directly proportional to the difference between impedance to be measured and the reference impedance, which is $4\Delta\alpha/K$. This feature can be used to increase the modulation index significantly.

4.7 Microcontroller

The schematic diagram of the microcontroller (U8) connections with other peripherals is shown in Figure 4.9.The microcontroller U8 is “Microchip PIC24FJ64GB004” [22], a 16-bit processor with 44-pin TQFP package. It has 64K byte program flash memory and 8K byte data RAM. It can be operated with a power supply in the range of 3.0–3.6 V. Typical current consumption is 2.9 mA at 3.3 V supply with the clock of 4 MHz. In our design, it is operating at 3.3 V. The maximum clock frequency (F_{osc}) supported by this IC is 32 MHz and the instruction clock is half of the system clock (16 MIPS). The system clock can be generated on-chip by an internal RC oscillator and PLL thus eliminating the use of an external crystal. Fast internal oscillator (FRC) with a nominal 16 MHz clock has been used. To stabilize the

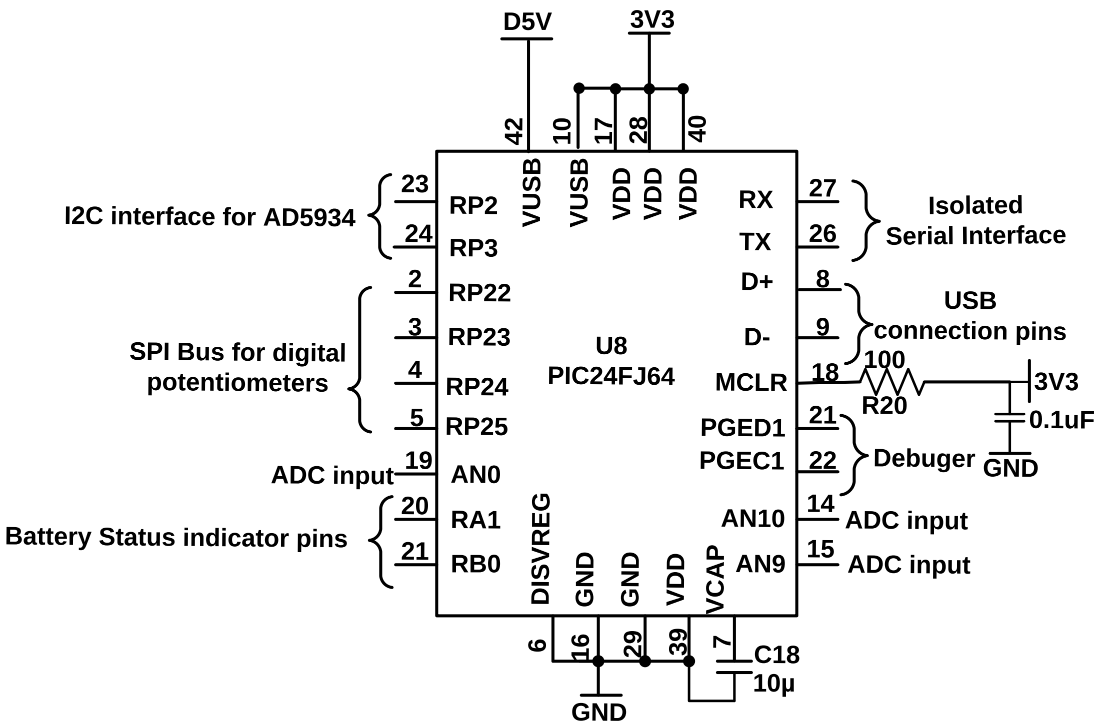

Figure 4.9 Microcontroller circuit (U8: PIC24FJ64GB004)

output voltage of the on-chip voltage regulator, capacitor C18 of 10 μF is used. All the capacitors near to VDD and VSS are connected at a distance less than 6 mm from the pins. PGEC and PGED pins are used for in-circuit serial programming and debugging. Microcontroller has two I2C modules which support multi-master/slave mode and 7-bit/10-bit addressing. One of the I2C modules is used to communicate with AD5933. It also consists of 3 SPI modules supporting 8-bit and 16-bit data frame operating at clock frequencies up to 16 MHz, one of the SPI modules is used to control the two digital potentiometers. The ADC has 10 analog input channels having 10-bit resolution and with a maximum of 500 kHz sampling rate. Three channels are used. It also has two on-chip UART modules. One of them is used to communicate with the PC as described in Section 4.8.

4.8 Isolated serial interface

The instrument is designed to be battery powered; to eliminate any connection of the instrument to the AC mains. This reduced the pickups and ensures the medical safety of the patients from electrical shocks. UART 1 module of the microcontroller is used to communicate with the PC. The circuit is isolated from the PC by using IC “Analog Devices ADM3251E”. This electrical isolator IC has 2.5 kV isolation and single channel transceiver-cum-isolator operating at a single supply of 5 V (dc-dc converter enabled) or 3.3V (dc-dc converter disabled) on primary side and supports data rate up to 460 kbps [23]. On the secondary side, power is provided by the internal charge pump which generates RS232 levels

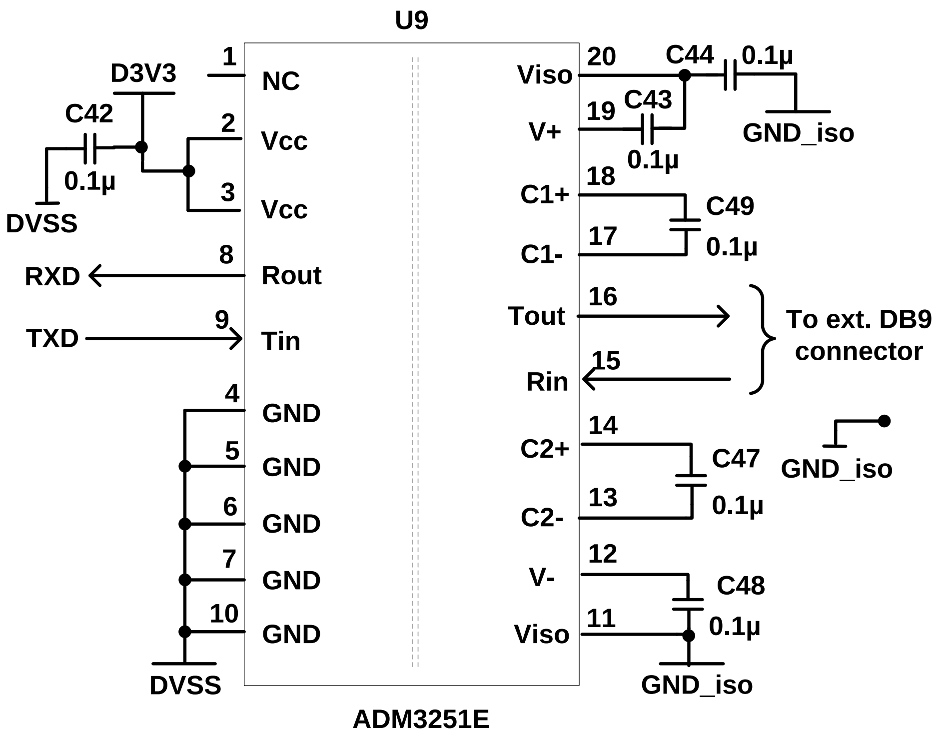

Figure 4.10 Serial isolated interface

using four external 0.1 µF capacitors (C20, C22, C23, and C24). Secondary side can also be powered by 5 V USB from a PC port to reduce the power consumption. This option has been used in our design. The internal dc-dc converter is disabled, and it reduces the current consumption from 140 mA to 12 mA. Figure 4.10 shows isolated serial interface using ADM3251E as U9.

4.9 Power supply

Impedance converter U1 and microcontroller U8 use separate power supplies for analog and digital blocks, hence two separate regulators have been used to reduce coupling between digital and analog blocks. The power supply circuit is shown in Figure 4.11. Total current consumption of the overall circuit is estimated by considering current requirements of the individual chips. Total current consumption of the circuit for analog and digital supplies are estimate as follows.

D5V5 (digital 5 V): 7 mA (U9:1 mA, U13:1 mA, U1: 3 mA, U8: 2 mA)

A5V5 (analog 5 V): 15 mA (U4: 6 mA, U5: 6 mA, U6: 2 mA, U18: 1 mA)

D3V3 (digital 3.3 V): 32 mA (U8: 12 mA, U1: 10 mA, U6: 2 mA, U9: 8 mA)

A3V3 (analog 3.3 V): 6 mA (U1:5 mA, U17: 1 mA)

Thus the total current consumption is calculated to be approximately 60 mA. Analog reference of 1.65 V is generated from analog 3.3 V to get the bipolar voltage swing around

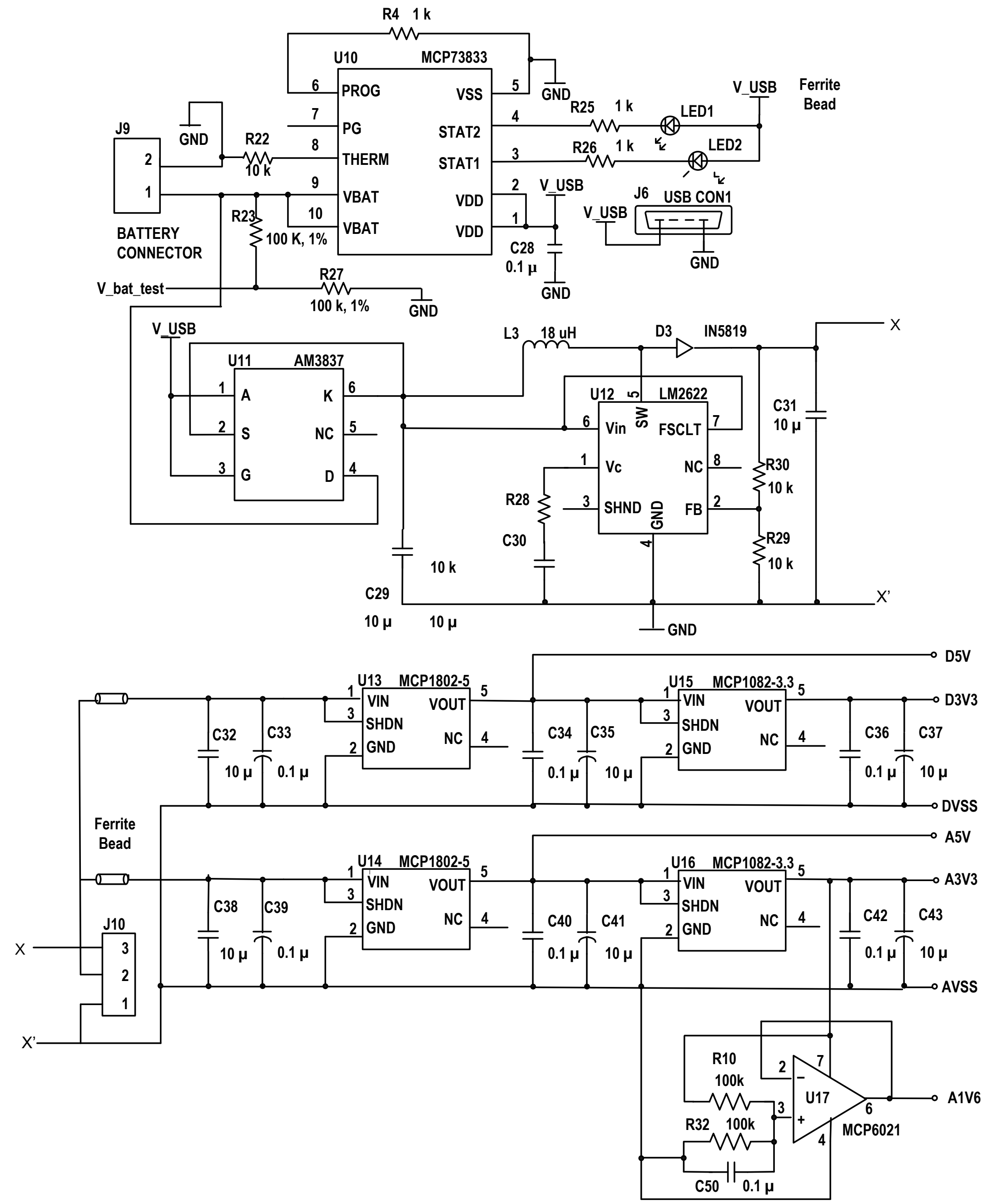

Figure 4.11 Power supply circuit

1.65 V as the on-chip ADC of the impedance converter and the microcontroller operate at 3.3V. In the figure analog 5.5 and 3.3 supplies are labeled as A5V and A3V3, respectively. The digital 5V and 3.3V supplies are labeled as D5V and D3V3 respectively. Analog and digital grounds are labeled as AVSS and DVSS, respectively. Analog reference voltage of 1.65V is labeled as A1V6. To obtain 3.3 V analog and digital supplies, two low dropout linear regulators ICs U15 and U16 are used. “MCP 1802-3.3” [28] has been used as U15 and U16. Its input voltage range is 3.6 - 10V and has very low quiescent of 25 µA. The analog 3.3 V is obtained from analog 5 V and digital 3.3 V is obtained from digital 5 V. Thus the current regulators for analog and digital 5 V are 21 mA and 39 mA, respectively. To obtain 5 V power supplies another set of low dropout linear voltage regulators “MCP 1802-5” [28] have been used as U13 and U14, its input range lies between 5.3 to 10 V and it also has quiescent current of 25 µA. Thus the circuit can be powered by a single dc voltage of 5.3-10 V, with 60 mA current capacity.

To power the circuit from a Li-ion battery of 3.6-4.2 V or from USB power source, a dc-dc converter “TI LM2622” [29] is used as U12. It is a step-up dc-dc converter with a 1.6 A, 0.2 Ω internal switch and pin selectable operating frequency. It can be operated at switching frequencies of 600 kHz and 1.3 MHz, with the ability to convert 3.3V to multiple outputs of 8V, -8V, and 23V. A MOSFET switch U11 is provided to switch the power mode automatically. When USB power is present the circuit will be powered through USB supply, and when it is absent the circuit will be powered by battery. Charging facility also has been provided by using a standalone linear Li-ion controller “Microchip MCP 73833” as U10 with maximum output of 500 mA. LED1 indicates that the battery is charging and LED2 indicates full charge. Battery voltage is monitored by on chip ADC of microcontroller through one of its analog input pin. At present the regulators are powered through standard dc regulated power supply, dc-dc converter and U10, U11, and U12 are yet to be soldered and tested.

4.10 PCB design and system assembly

A two-layer PCB with PTH has been designed for the circuit. Most of the components used are in SMD package and they have been mounted on both the layers to reduce the number of track crossovers and the overall size of the board. The final size of the board is 102 mm x 64 mm. Wherever needed, the top and bottom side tracks have been connected by 0.8 mm diameter PTH having. Since the PCB contains analog as well as digital blocks, separate analog and digital power and ground planes have been used to avoid noise problems. The analog ground and digital ground are routed separately throughout the board and are shorted at the input power supply. The power supply pins of all the ICs have been decoupled using 0.1 µF capacitors at maximum distance of 6 mm from the IC. Digital 5 V, digital 3.3 V, analog 5 V, analog 3.3 V have been distributed as separate planes on the top side of the board. Similarly, digital and analog ground planes have been provided on the bottom side of the PCB. Shortest overall connection path have been chosen for pin-to-pin connections.

The minimum signal track width used is 0.25 mm and the width of the power line tracks is 1.27 mm. A minimum clearance of 0.25 mm has been used between two signal tracks and between a signal track and polygon plane. A 45^{o} corner style has been used for routing corners. The different hardware blocks of the instrument have been separated using

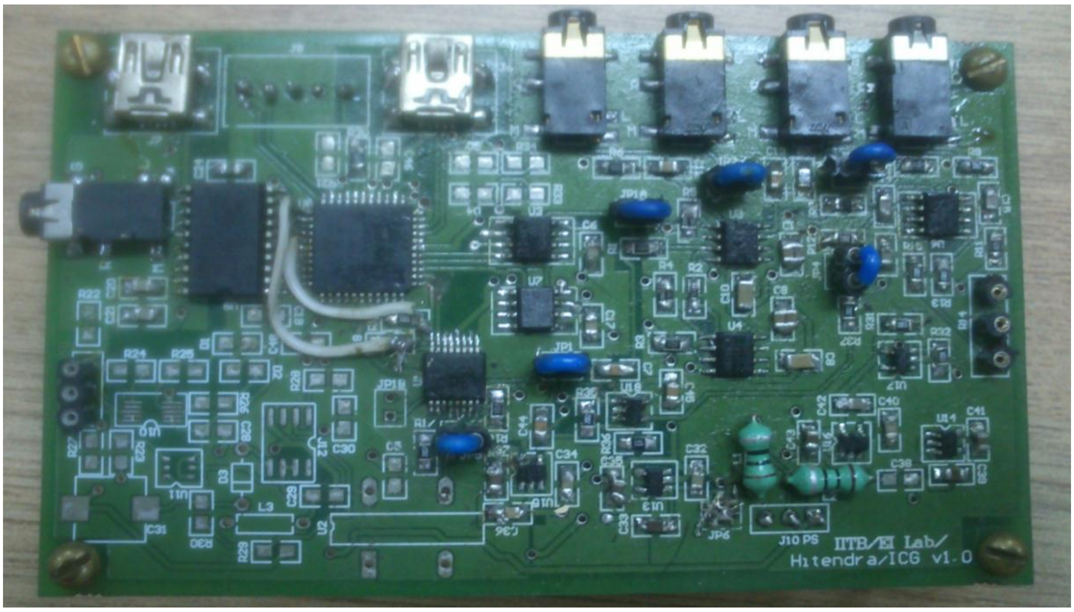

Figure 4.12 Top view of assembled PCB

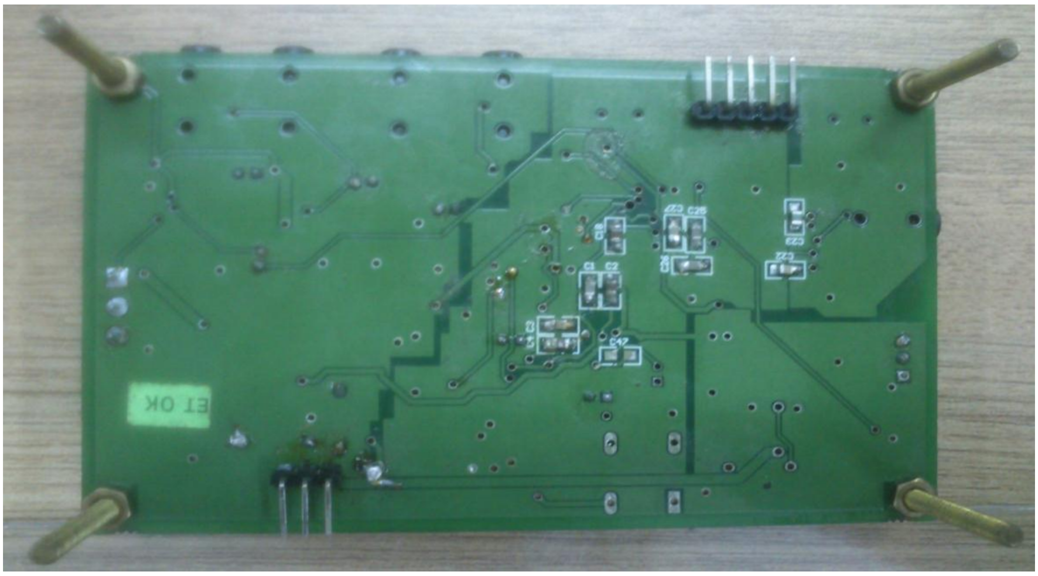

Figure 4.13 Bottom view of assembled PCB

jumpers so that they can be tested individually. The circuit schematic and the PCB layouts (top layer, top overlay, bottom layer, bottom overlay) are given in Appendix A and B.

Before assembling the components on PCB, a check on all the tracks was carried out to ensure continuity and also to verify that there were no shorts between any neighboring track pairs. All components were soldered manually care taken not to exceed maximum lead temperature ratings for SMD packages. After assembling the components, the PCB was thoroughly examined to ensure there were no shorts between IC pins due to formation of solder bridges and again a continuity check was performed to avoid the possibility of dry solder. The different hardware blocks were then tested separately to ensure their proper operation. Two sides of the assembled PCB are shown in Figure 4.12-13.

4.11 Microcontroller program

Program "icg_main" for the microcontroller PIC24FJ64GB004 is written in embedded C using "Microchip MPLAB IDE". The microcontroller has internal power-on reset and starts with internal default oscillator as the clock source. The clock configuration bits are used to select the internal FRC oscillator with clock frequency of 16 MHz as the clock source. Next all the I/O pins are configured by programming appropriate TRIS and PORT registers. I2C, SPI, UART, ADC and Timer modules of the microcontroller are initialized by the main program. Impedance converter IC AD5933 is initialized to configure data rate and clock frequency. Timer 3 is used as a 16-bit timer, and Timer 4/5 is used as a 32-bit timer.

Timer 3 is used to set the sampling frequency of the on-chip ADC of the microcontroller for sampling (i) the output of the voltage sensing amplifier (Vout of U6 in Figure 4.7) for sensitivity adjustment and (ii) output of the summing amplifier (Vo of U18 in Figure 4.8) for baseline correction. The sampling rate f_s is set by loading Timer 3 with an appropriate digital count N_{timer} which is calculated as

$$N_{timer} = F_{clk}/f_s \tag{4.21}$$

where F_{clk} is the clock frequency of the microcontroller. With F_{clk} = 16 MHz, we set f_s = 500 kHz, by using N_{timer} = 32 as 16-bit count. Timer 4/5 is used to set the sampling frequency for the impedance measurement. Sampling rate for impedance measurement is set using the same formula. For setting the rate as 100 Hz, we load N_{timer} = 160000 as 32-bit count.

The excitation current amplitude is set to the most appropriate value by monitoring the sensed voltage. Sensed voltage signal is sampled by the ADC of the microcontroller and compared against a predefined threshold level inside the microcontroller. If this voltage is below the defined threshold limits the count of the digital potentiometer U3 is increased in order to increase the input to the V-to-I converter; it will increase the excitation current flowing through the unknown impedance. And if this voltage is above the threshold limits then by decreasing the count of the digital potentiometer U3 the current excitation is lowered. This achieves automatic sensitivity settings with the optimum value of excitation current set, for different values of the thorax impedance.

The sensed signal is passed to the baseline correction circuit, and the output of the baseline correction circuit is also sampled in order to compare it with the predefined threshold to prevent the saturation of the ADC input of the impedance converter AD5933. Digital potentiometer U7 ratio is varied between the 0.25 to 0.75 to keep the signal amplitude within the predefined threshold limits. The signal gets demodulated and data samples are stored in

the impedance data registers. Status register is polled continuously to know whether the measurement is completed. When the impedance data samples are available, these data samples and the corresponding values of the digital potentiometers are sent to the PC. These impedance data values and the values of the digital potentiometers (U3 and U7) ratios are stored in a text file. These values are used in the calculation of the unknown impedance. Another microcontroller program "icg_temp" is written for testing purpose. This program calculates the unknown impedance in the microcontroller itself and the impedance data can be outputted directly from an array to the file using either "MPLAB IDE" or hyper terminal.
The algorithm of "icg_main" can be described as following.

Main program

1. Configure the FRC oscillator for 16 MHz.
2. Set TRIS and PORT registers for I/O operation.
3. Configure serial port for data transfer.
4. Configure Timer 3 for ADC sampling frequency of 500 kHz and Timer 4/5 for measurement rate of 100 Hz.
5. Set the default values of digital potentiometers U3 and U7.
6. Wait for the interrupts in an indefinite loop.

Interrupt Service Routine for Serial Port

1. Decode the received byte and go to the appropriate step.
2. *"$": Check device status.* Initialize the AD5933 and poll for successful communication. Send "#" character to the PC. Program frequency registers of AD5933 for 65.56 kHz. Return.
3. *"*": Start Acquisition.* Turn on the ADC, Turn on timer 3. Return.
4. *"@": Stop Acquisition.* Stop timer 5 and close the serial port. Return.

Interrupt Service Routine for Timer 3

1. Check the baseline flag "flag1". If it is not set, continue in the sensitivity setting mode. Read one sample of Vout of U6 (Figure 4.7). Increase the count variable and check whether 400 samples have been acquired. If 400 samples are not acquired then return to the main program and do not execute the remaining code. It may be noted that the sampling interval gets determined by the count loaded in Timer 3. If 400 samples have been acquired, find the maximum and minimum values of the acquired samples. Compare the peak-to-peak value with the specified thresholds to keep the output within the limits to prevent its saturation. If the values are too large, change the digital potentiometer U3 count to decrease its output. If the values are too small, change the count to increase the output. If the values are within the thresholds, treat

the sensitivity setting operation is as finalized. Set the flag variable “flag1” for baseline correction signal sampling.

2. If the baseline signal flag “flag1” is set then operation like step 1 is repeated for baseline correction, by reading 400 values of V_o of U18 (Figure 4.8) and changing the count of U7.
3. Disable Timer 3, and enable Timer 4/5 for setting the measurement rate as 100 Hz.
4. Return to the main program.

Interrupt Service Routine for Timer 4/5

1. Give start measurement command to the AD5933.
2. Poll the status register of AD5933 for the completion of the measurement.
3. Read measured real and imaginary values from AD5933.
4. Send these measured values to the PC over RS232 interface.
5. Return to the main program.

4.12 PC program for impedance data acquisition

A PC-based graphical user interface (GUI) program is developed in LabWindows CVI for impedance data acquisition and is named as “ICG_DAQ”. It can be invoked by clicking on the executable file (.exe). It can be used for acquiring and storing the real and imaginary parts of the impedance measurements from the serial port of the ICG instrument. The serial communication is at the baud rate of 115,200. In case PC does not have a serial port, a USB-to-serial converter may be used.

The program operates by interacting over the serial port with the microcontroller of the ICG instrument, as described earlier in Section 4.11. The PC program has four buttons: Check Device Status, Start acquisition, Stop Acquisition, Plot Z Waveform. Figure 4.16 shows a screenshot of the GUI for the data acquisition.

On pressing of “Check Device Status”, program checks the serial port connection and working of the ICG instrument. It sends the character “$” over the serial port. If “#” is received as response from the microcontroller, “Device is ready to use”, message is displayed, and “AD5933 Error” message is displayed otherwise. After receiving “$”, the microcontroller program initializes AD5933 and reads its status register. If the status register is read successfully, it replies to the PC by sending “#”. Thus receiving this character indicates, proper functioning of serial connection between PC and ICG instrument and also the communication between the microcontroller and AD5933 inside the ICG instrument.

At the press of “Start Acquisition”, the character “*” is sent over the serial port. The program expects to receive the measured values as 17 bytes of data, with measurements carried out by the ICG instrument at a sampling frequency of 200 Hz or lower as set in the microcontroller program. After receiving 17 bytes of data, the serial input buffer is reset to

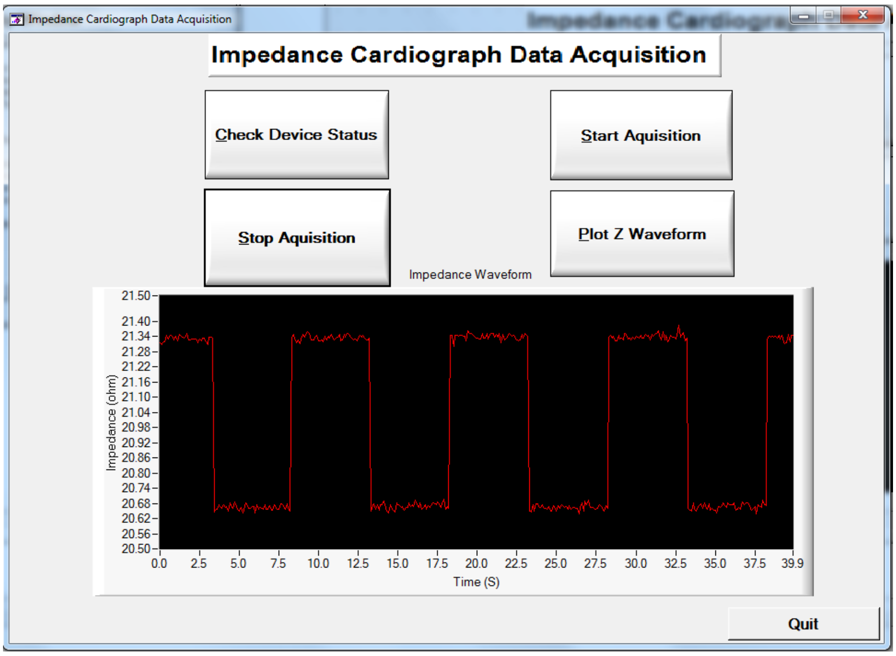

Figure 4.16 Screenshot of the impedance cardiograph GUI

receive the next set of bytes. The received data are stored in an array of 10,000 samples. If the array gets filled, the serial port is closed, and the program waits for pressing of "Stop .Acquisition" or any other button. The operation on the microcontroller side has been described earlier in Section 4.11. After receiving the character "*" over the serial port, the microcontroller starts periodic measurement mode at a sampling frequency of 100 Hz. After each measurement, i.e. every 10 ms, it sends the 8 bytes of the real part, "#" as separator, and 8 bytes of imaginary part. At the press of "Stop Acquisition", the program sends the character "@" to the microcontroller. In response to receiving this character, the microcontroller program stops the timer 4/5, and closes the serial port. The samples acquired in the array are stored in a text file "Z.txt" in the current folder, overwriting any pre-existing file. The stored data will have the acquired samples and the rest will be zero valued, because the buffer is initially filled with zeros.

Press of "Plot Z waveform" button leads to plotting of the impedance waveform from the stored data file "Z.txt".

Chapter 5

TEST AND RESULTS

5.1 Voltage sensing amplifier output

For testing the operation of circuits for excitation and voltage sensing, the excitation frequency was set at 65.56 kHz. The digital potentiometer U3 ratio was set at 0.40 to get the excitation current of 0.9 mA (p-p). The potentiometer of R15 in the circuit of Figure 4.7 was adjusted to set the gain of the voltage sensing amplifier as 10. To check the linearity, different test resistors were connected across the terminals I1 – I2 and the voltage developed across the terminals E1- E2 was measured. Table 5.1 shows the output V_O of voltage sensing amplifier corresponding to the different resistances. Figure 5.1 show a relationship between the two is almost linear. It was found that the linearity was valid for the resistance up to 400 Ω for an excitation current of 0.9 mA.

Table 5.1 Voltage sensing amplifier output for different test resistances

Resistance (Ω) between I1-I2	V_O (mV) across E1-E2
10	88
20	168
30	250
40	330
50	420
60	504
70	580
80	656
90	744
100	840
110	912
120	1000

5.2 Automatic sensitivity adjustment

The design has an automatic sensitivity setting feature. It is implemented by setting the excitation current amplitude such that the output of the voltage sensing amplifier is within the specified limits, so that the input to the ADC does not saturate and is not too low. This is

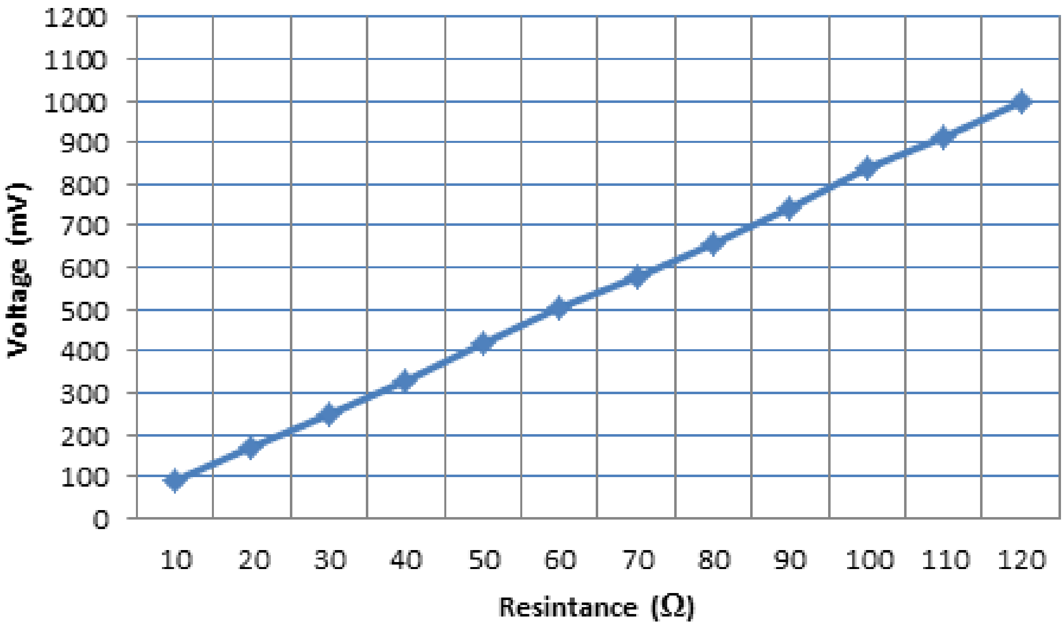

Figure 5.1 Plot between Voltage sensing amplifier output and test resistances

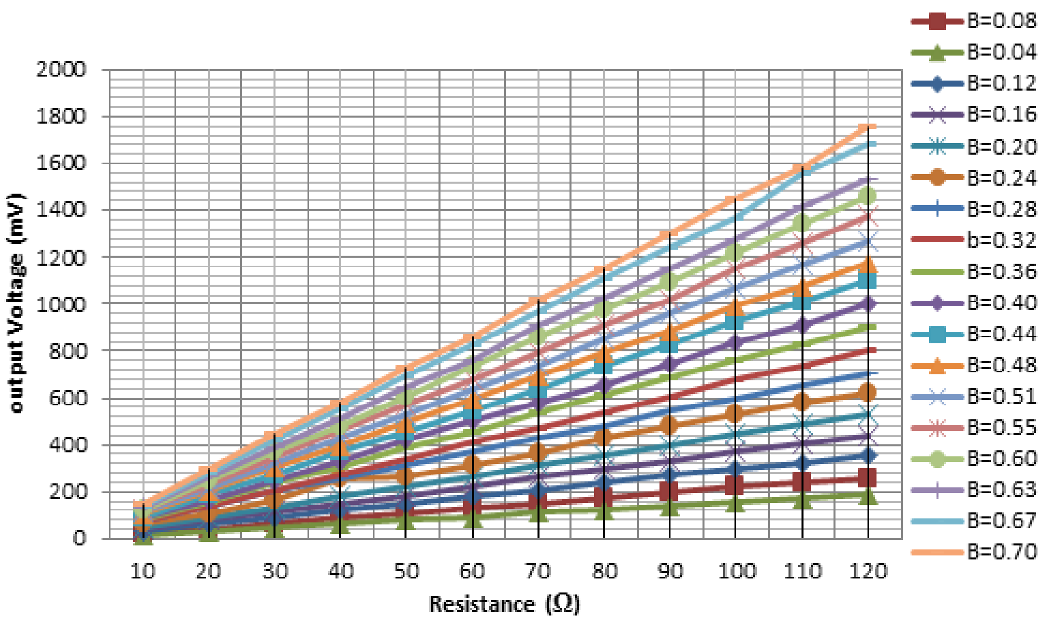

Figure 5.2 Plot between Voltage sensing amplifier output and test resistances for different values of the current set by varying ratio β.

achieved by changing the potentiometer ratio of U3 as $0.24 \leq \beta \leq 0.7$. If β is increased beyond 0.7, the output of the V-to -I converter gets distorted.

For this range of β, current varies between 0.6 mA and 1.75 mA. The output of the voltage sensing amplifier is monitored continuously using on-chip ADC of the microcontroller till it sets the maximum allowable current without saturating the input of the ADC. To check the linearity for all possible values of the current, different test resistances were used. Gain of the voltage sensing amplifier was 10 as in the previous test. Figure 5.2 shows the graph between the test resistance and measured output voltage for different values of β.

5.3 Validation of the hardware using impedance simulator

The developed hardware was tested with the thoracic impedance simulator which is described in Chapter 3. Impedance simulator generates time-varying impedance signal in the form of variation in the resistance over the basal resistance. The frequency of sinusoidal excitation was set as 65.5 kHz. The potentiometer U3 ratio was set at 0.24 to get an excitation current of 0.6 mA (p-p). The current injecting and the voltage sensing terminal pairs were shorted and connected to the terminals E1 and E2 of the impedance simulator. The gain of the voltage sensing amplifier was set at 10 as in the previous two tests. The gain of internal amplifier of the impedance converter chip was programmed to be 5. The output of the voltage sensing amplifier is directly given to the AD5933 by bypassing the baseline correction circuit. The demodulator output in the form of real and imaginary numbers corresponding to the unknown impedance were calculated at the sampling frequency of 100 Hz. Sampling frequency for the measurement of unknown impedance is set by using the timer 4/5 of the microcontroller. These data were acquired through the PC based GUI over RS232 interface and stored in a text file. For calibration, the values were also recorded by connecting a known resistance of 30 Ω across the excitation terminals. These values were used to compute a calibration factor. This factor was used to convert the demodulator output values from the impedance converter chip to impedance values, using (Eq. 4.8) as given in Section 4.2.

Table 5.2 Impedance simulator settings for the outputs shown in Figure 5.3 – 10

Figure	R (Ω)	ΔR (Ω)	F (Hz)
5.3	20	0.8	0.1
5.4	30	1	0.3
5.5	30	0.2	0.5
5.6	30	1	0.5
5.7	49	0.5	1
5.8	19	0.2	1
5.9	19	0.5	5
5.10	98	1	5

The impedance simulator provides a time-varying resistance across its terminals, in the form of a small step variation over a basal resistance at the specified frequency corresponding to the heart rate. The simulator settings used for testing are given in Table 5.2. Figures 5.3-10 show plots of the time-varying measured values. It is seen that the step changes introduced by the impedance simulator are correctly reflected in the measured values. By observing these waveforms, the peak ripples in the measured values are found to be less than 0.08 Ω.

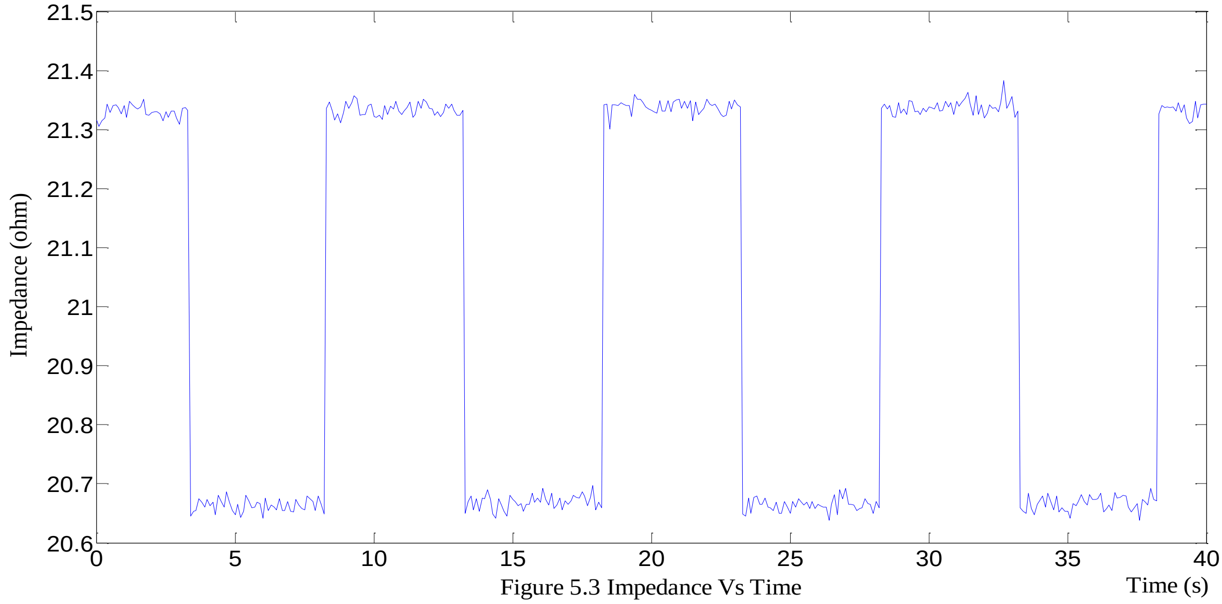

Figure 5.3 Impedance Vs Time

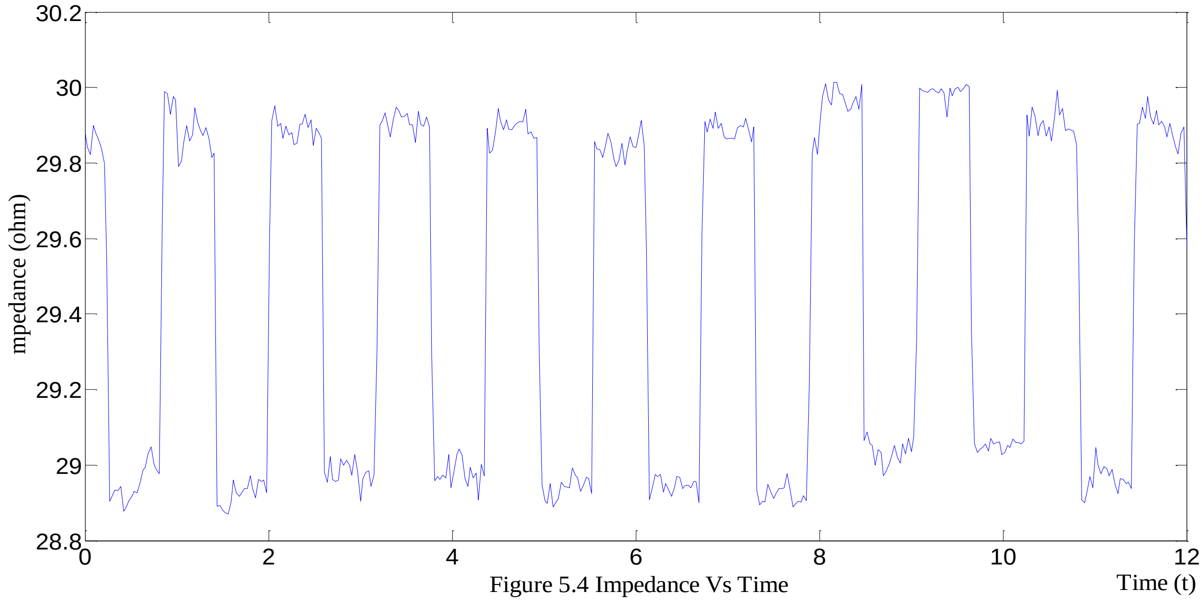

Figure 5.4 Impedance Vs Time

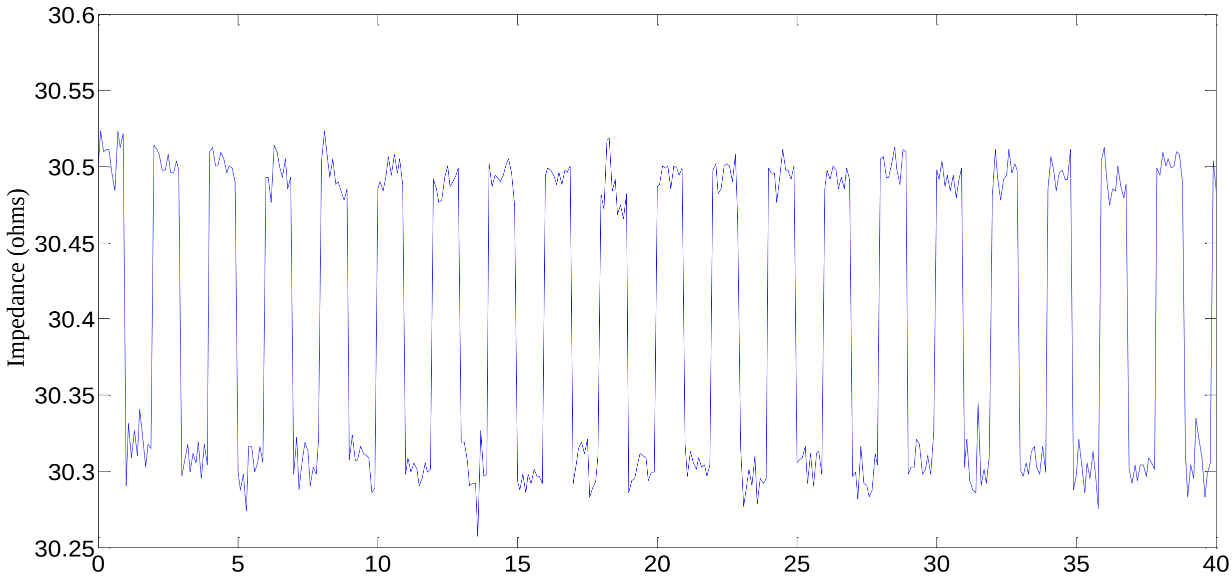

Figure 5.5 Impedance vs Time

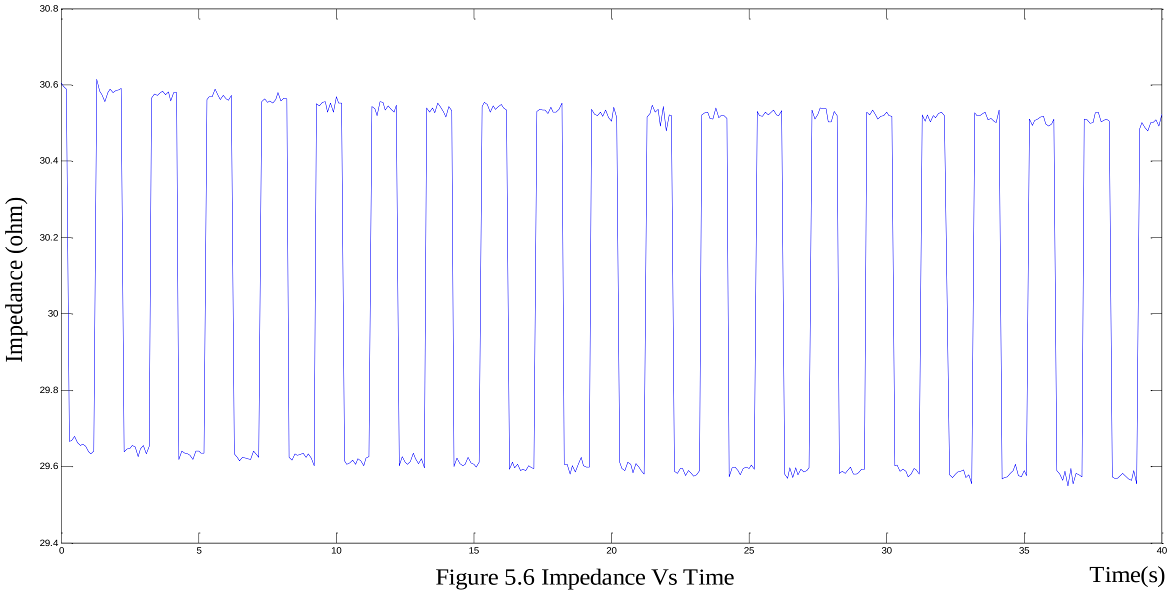

Figure 5.6 Impedance Vs Time

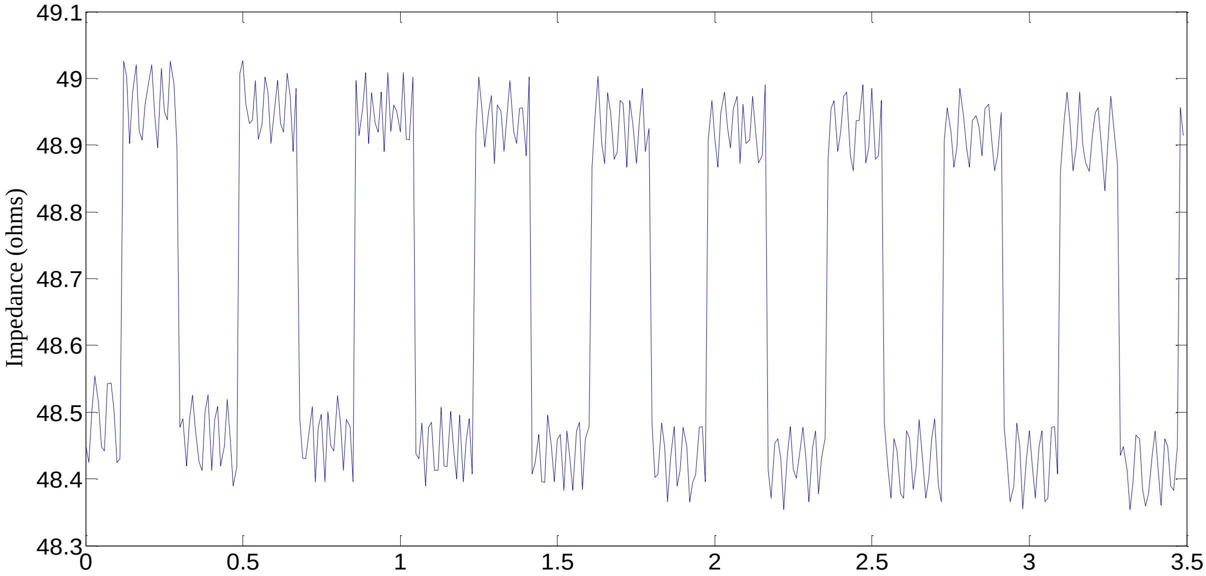

Figure 5.7 Impedance Vs Time

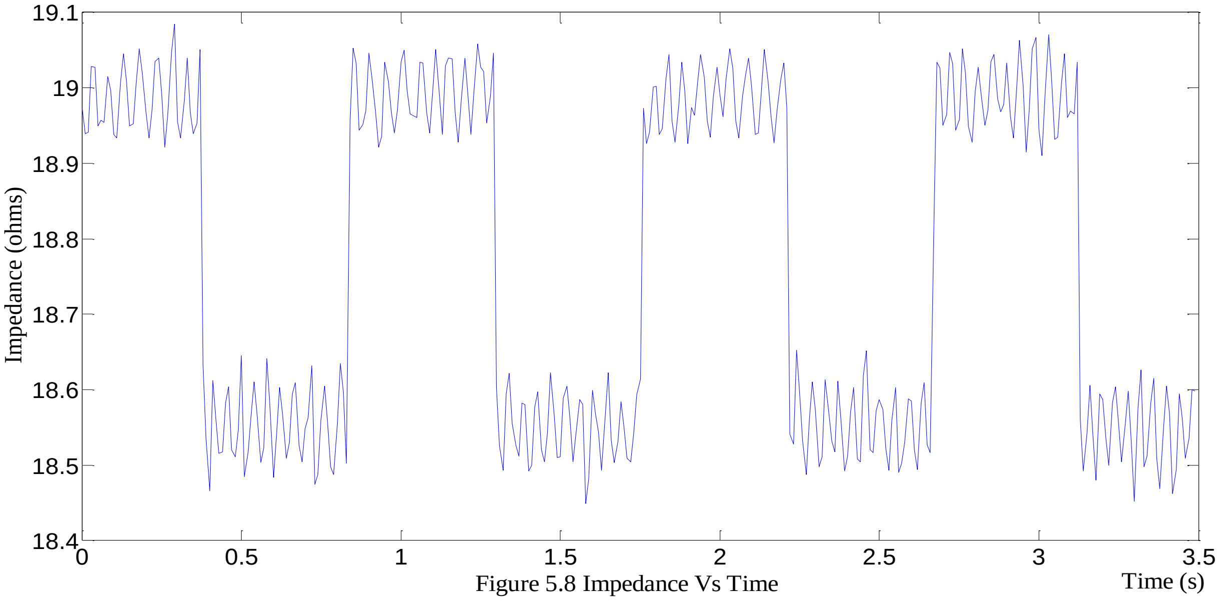

Figure 5.8 Impedance Vs Time

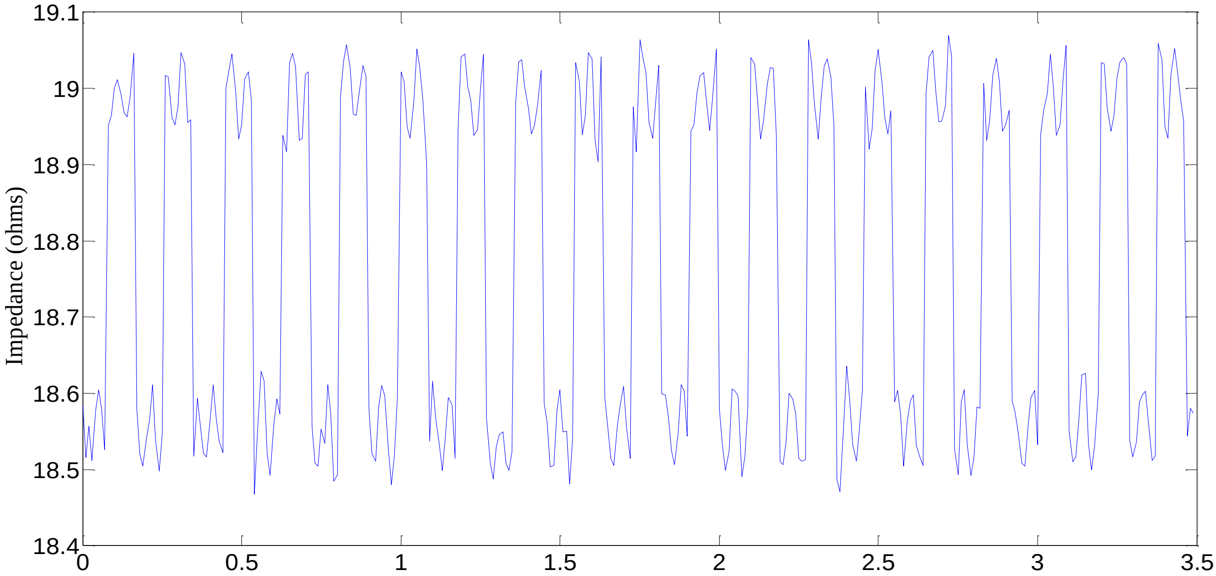

Figure 5.9 Impedance Vs Time

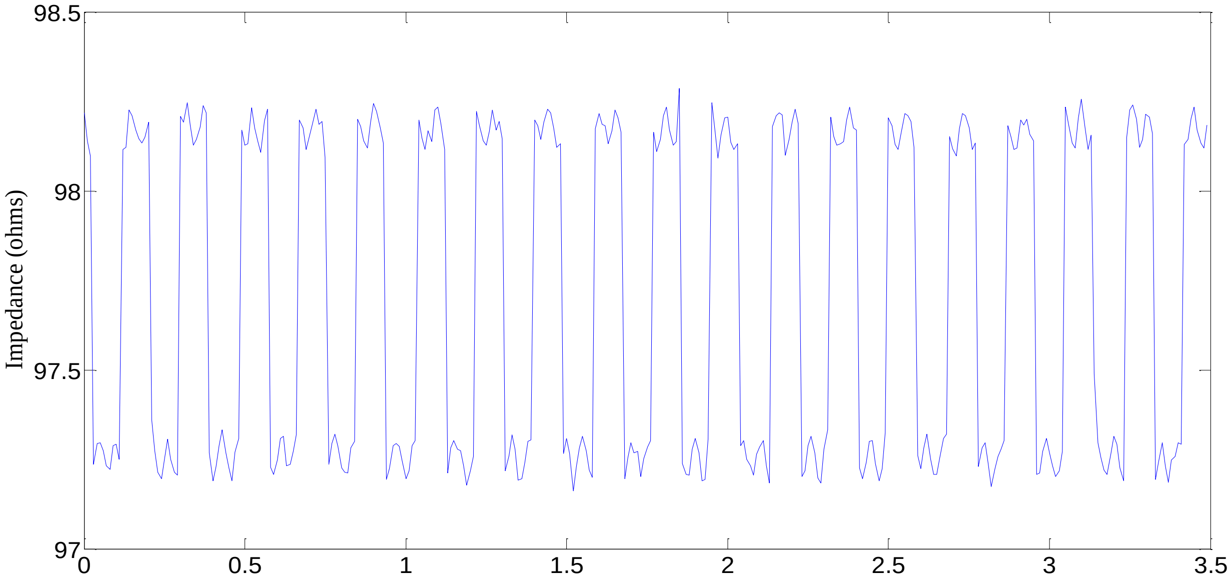

Figure 5.10 Impedance Vs Time

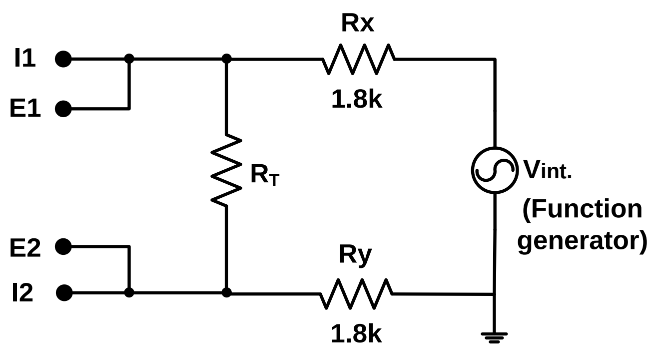

Figure 5.13 Noise rejection testing circuit

5.4 Noise rejection

Noise rejection by the hardware was tested by introducing current at different frequencies for a 20 Ω, test resistance (R_T), as shown in Figure5.13. The excitation current frequency was set at 65.56 kHz. The interference voltage amplitude was set to 500 mV (p-p) for the excitation currents of 0 and 0.9 mA. The frequency of the interference voltage was varied from 1 kHz to 1 MHz. The impedance was measured for each interference frequency and the measured values are tabulated in Table 5.3. It is seen that the interference affects the measurement only if its frequency is near the excitation frequency.

Table 5.3 Impedance measurement at different interference frequencies for a 20 Ω test resistance
Excitation current = Iex, Interference voltage = Vint

Interference Frequency (kHz)	Iex = 0 Vint = 500 mV (p-p)	Iex = 0.9 mA Vint = 500 mV (p-p)	Iex = 0.9 mA Vint = 0
10.0	1.60	19.97	20.00
20.0	1.60	19.98	19.99
30.0	1.60	19.94	20.01
50.0	1.60	19.98	19.98
60.0	1.60	19.95	20.00
64.0	1.60	21.23	20.00
64.5	6.17	25.87	20.00
65.0	13.12	31.61	20.03
65.1	14.27	31.08	20.02
65.2	16.96	33.79	20.00
65.5	16.35	35.92	19.98
65.7	17.01	35.53	20.01
65.8	15.96	36.17	19.98
65.9	15.31	34.82	20.02
66.0	4.31	33.25	19.93
67.0	1.50	23.15	20.01
70.0	1.50	19.99	19.99
100.0	1.50	19.98	20.05
130.0	1.50	19.97	19.97
131.0	1.50	20.02	20.00
132.0	1.50	20.03	19.47
196.5	1.50	19.98	19.96
197.0	1.50	19.95	19.98
262.0	1.50	19.98	19.99
500.0	1.50	19.99	20.00
600.0	1.50	19.98	19.97
700.0	1.50	19.97	20.04
800.0	1.50	20.03	19.98
1000.0	1.50	20.01	19.89

Chapter 6

SUMMARY AND CONCLUSION

The project objective was to develop an impedance cardiograph using novel circuits for signal acquisition and demodulation. After studying earlier reported designs, a new instrument has been designed using an impedance converter IC AD5933. This IC provides a sinusoidal source with high amplitude stability. It has digital synchronous demodulator which can provide high noise rejection for impedance cardiography. The circuit is developed using impedance converter, microcontroller, digital potentiometers, operational transconductance amplifiers, and op-amps. The circuit is powered by a single 5.3 – 10 V dc. It has provision for powering by a chargeable 3.6-4.2 V Li-ion battery and also by USB power.

AD5933 generates the waveform of high amplitude stability and settable frequency. Operational transconductance amplifier (OTA) based current source has been developed to get balanced output for current excitation without using a transformer. A digital potentiometer is used to vary the amplitude of the excitation current to set the sensitivity for the thorax impedance measurement. Baseline correction circuit is implemented by using ADC of the microcontroller, a digital potentiometer, and a summing amplifier. The baseline correction is controlled using software. The impedance converter chip has an on-chip ADC and a 1024-point DFT module. ADC samples the sensed and amplified voltage signal and the 1024-point DFT is used for synchronous digital demodulation. It provides excellent rejection of offsets and noises in the sensed voltage waveform. It gives real and imaginary part of the complex impedance in 2s compliment format. A user interface is designed to acquire ICG data samples through an isolated RS232 interface. The real and imaginary parts are used to calculate the magnitude and phase of the time-varying impedance. The impedance signal can be acquired at a sampling frequency of up to 200 Hz.

The impedance cardiograph circuit has been assembled on a 2-layer PCB with PTH and tested. The hardware is tested on the bioimpedance simulator and results are satisfactory. The hardware needs to be boxed and detailed tests needs to be carried out before its clinical use.

Appendix A

SCHEMATIC DIAGRAM OF IMPEDANCE CARDIOGRAPH

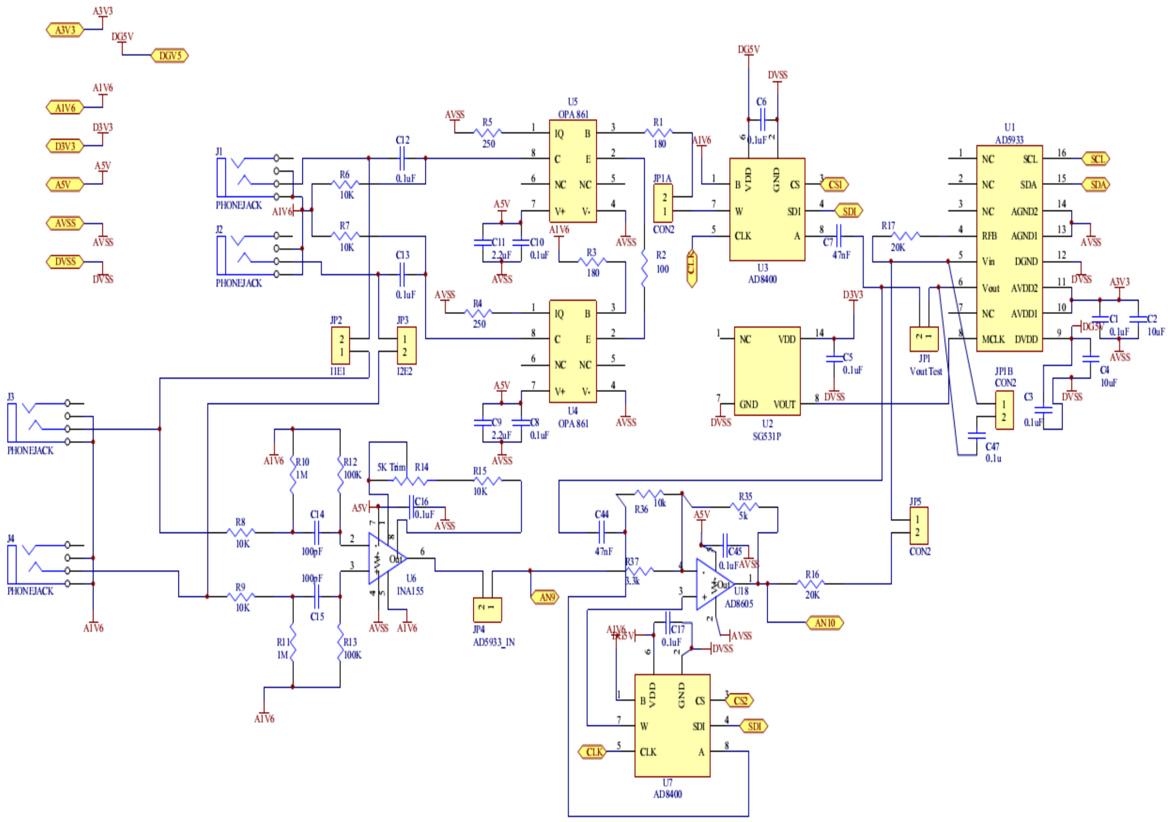

Figure A.1 ICG schematic sheet 1: Impedance converter, V-to-I converter and Voltage sensing amplifier.

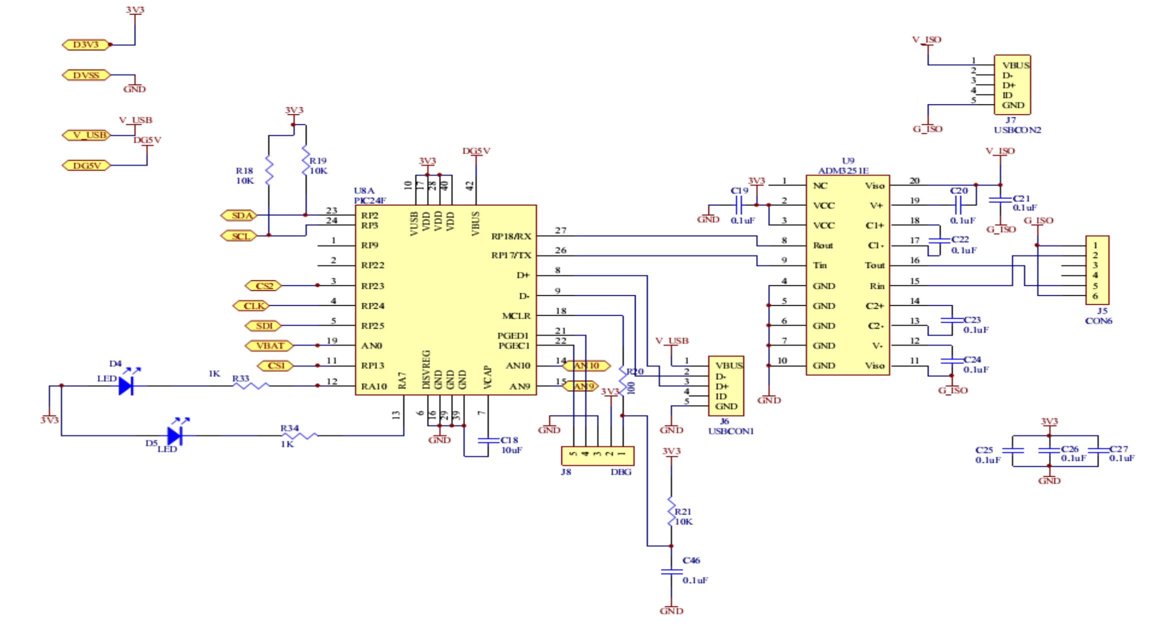

Figure A.2 Microcontroller and isolated serial interface

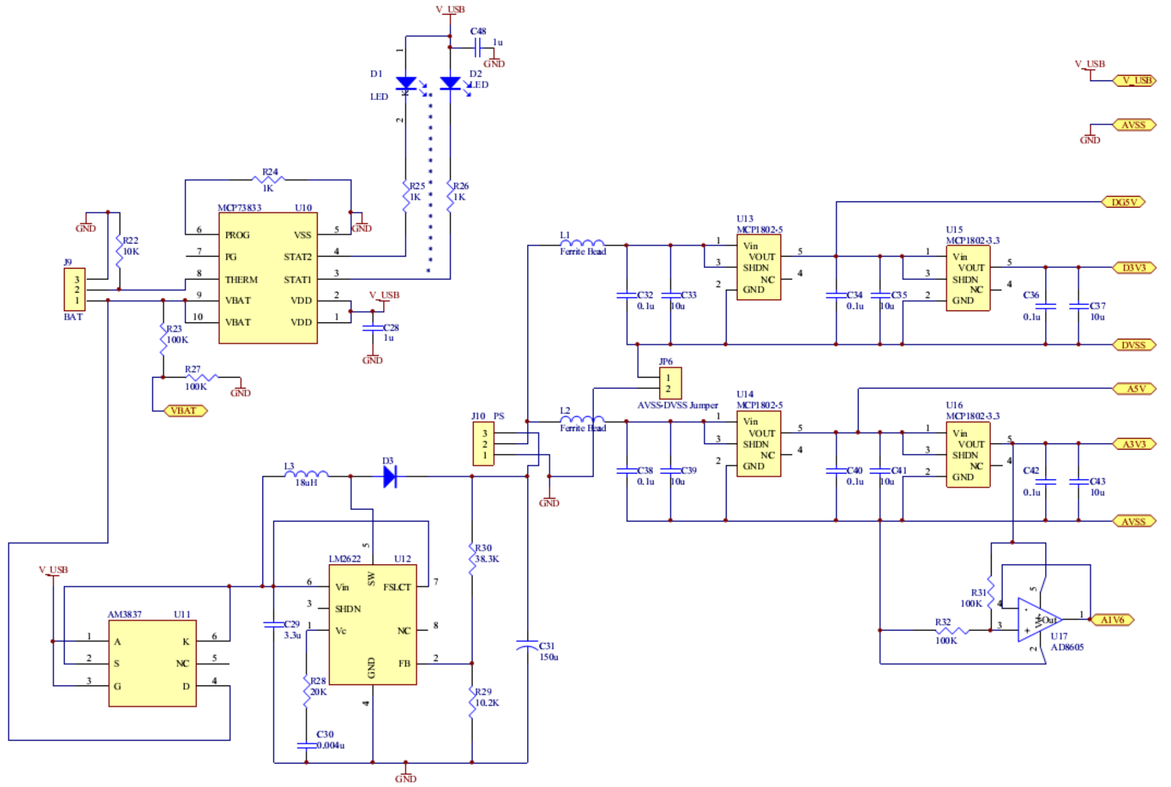

Figure A.3 Power supply Circuit

Appendix B

PCB LAYOUT OF THE IMPEDANCE CARDIOGRAPH

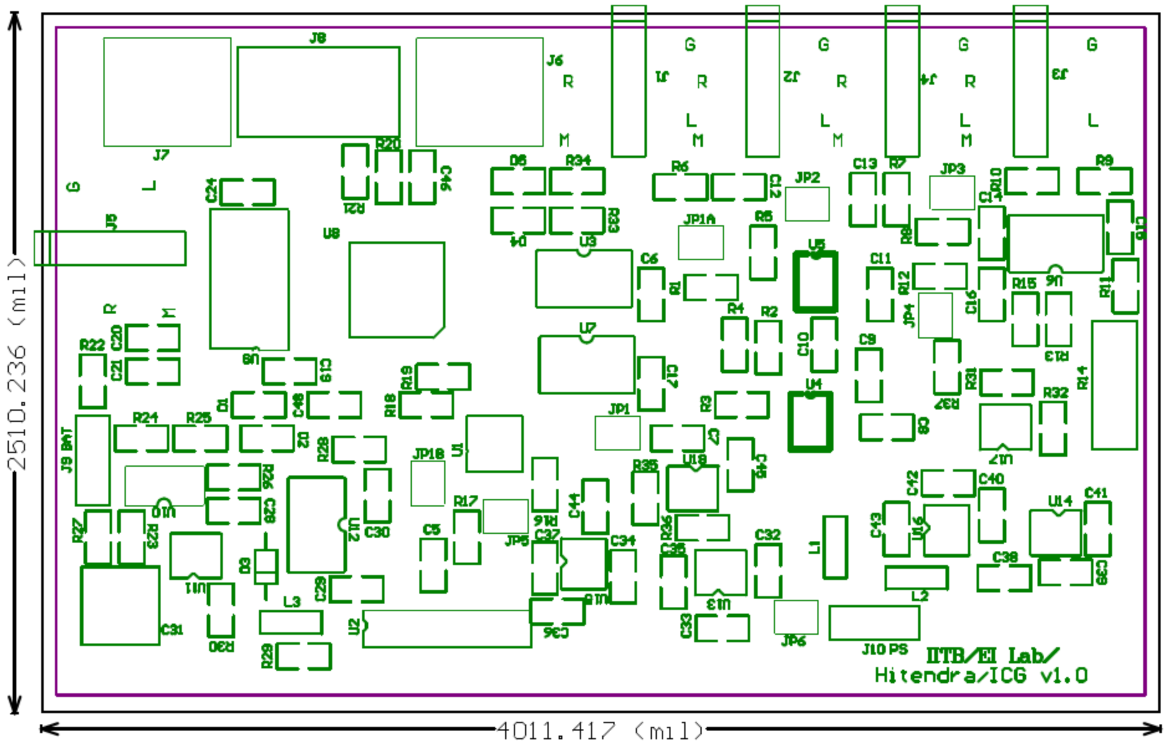

Figure B.1 Top overly of the assembled PCB

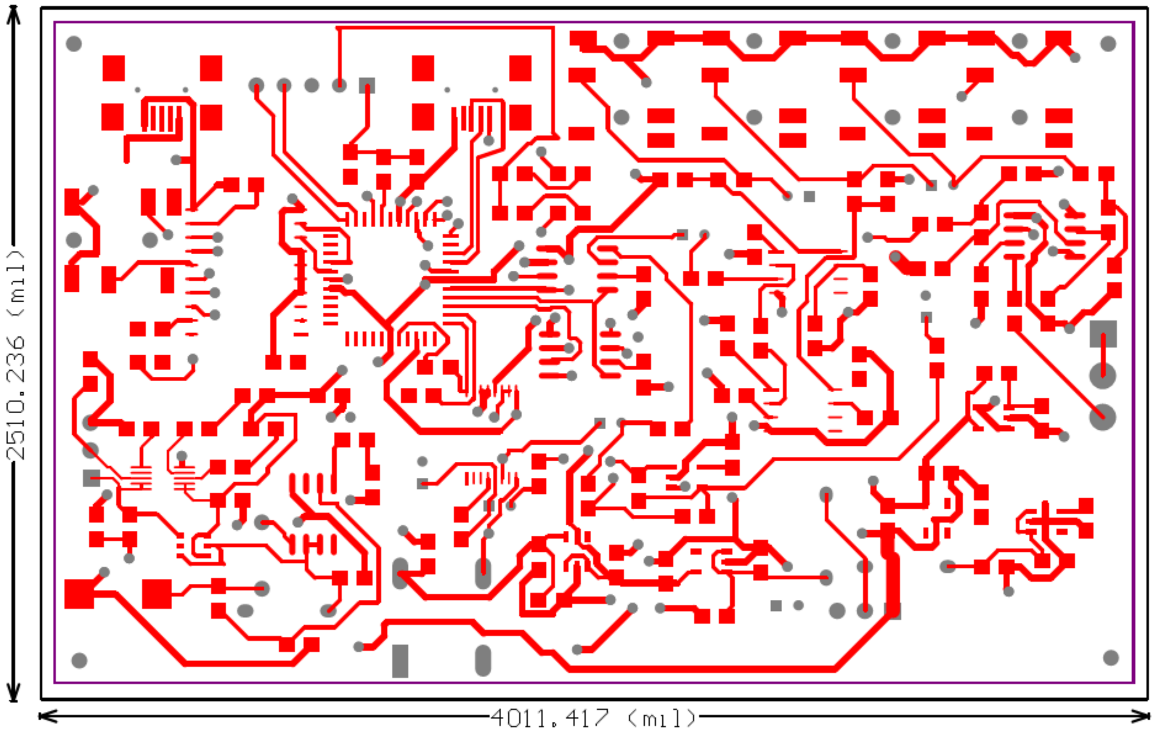

Figure B.2 Top layer of the assembled PCB

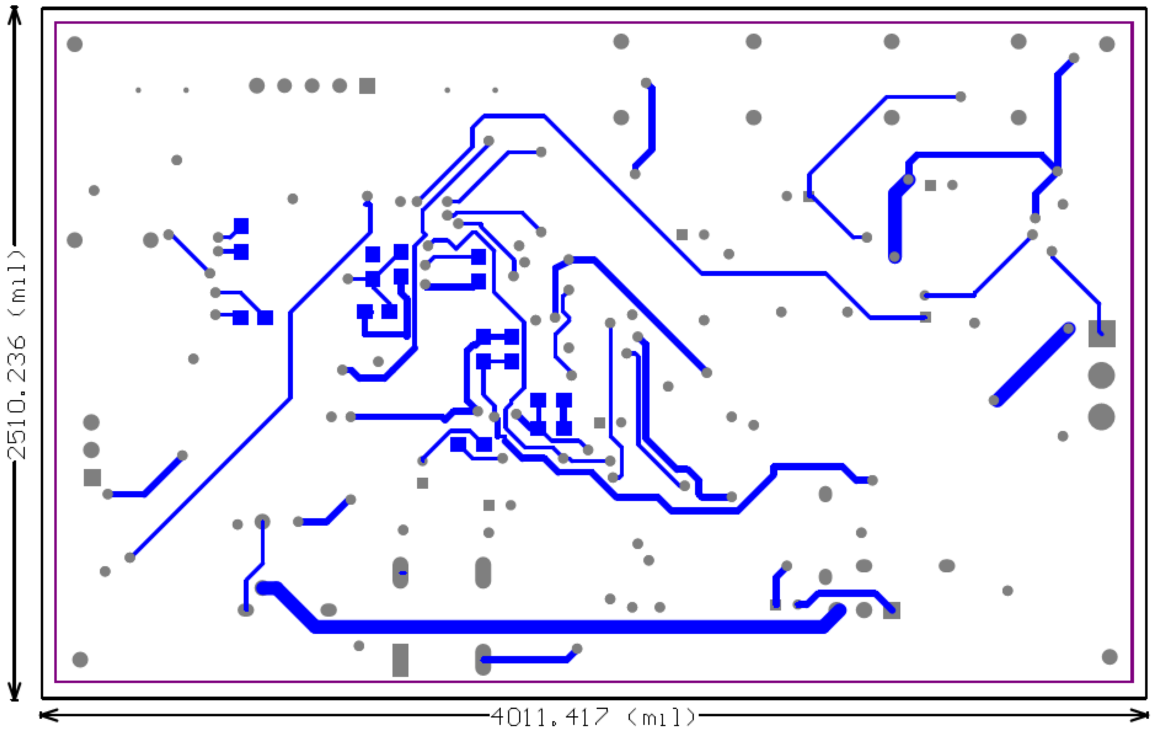

Figure B.3 Bottom layer of the assembled PCB

Appendix C

COMPONENT LIST FOR IMPEDANCE CARDIOGRAPH

Table C.1: Component list of the bio-impedance simulator

Component designator	Component description	Part Number /value	Quantity
C28, c48	Capacitor, ceramic, chip	1 μF	2
C34, C36, C38, C47, C32,			
C40, C42, C17, C6, C13,			
C27, C12, C16, C10, C3,			
C1, C45 C5, C20, C19,			
C24, C22, C23, C21, C25,			
C26, C46, C8	Capacitor, ceramic, chip	0.1 μF	28
C37, C33, C43, C39, C41,			
C35, C18, C4, C2	Capacitor, ceramic, chip	10 μF	9
C9, C11	Capacitor, ceramic, chip	2.2 μF	2
C29	Capacitor, ceramic, chip	3.3 uF	1
C7,C47	Capacitor, ceramic, chip	47 nF	2
C14, C15	Capacitor, ceramic, chip	100 pF	2
C31	Capacitor, ceramic, chip	150 uF	1
R6, R9, R7, R8, R19			
R21, R15, R22, R18	Resistor	10 kΩ	9
R34, R33, R25, R26			
R24	Resistor	1 kΩ	5
R29, R14	Resistor Trimmer	5 kΩ	2
R10, R11	Resistor	1 M	2
R16, R17, R28, R35, R37,	Resistor	20 Ω	5
R1, R3	Resistor	180 Ω	2
R4, R5	Resistor	250 Ω	2
R13, R31, R27, R23; R12,			
R32	Resistor	100 k	5
R2, R20	Resistor	100 Ω	2
U1	IC, Impedance converter	AD5933	1
U2	IC, oscillator	SG531P	1

U3, U7	IC, Digital Pot	AD8400	2
U4, U5	IC, OTA	OPA861	2
U6	IC, Instrumentation Amp.	INA155U	1
U8	IC, Microcontroller	PIC24FJ64GB004	1
U9	IC, RS232 driver	ADM3251E	1
U10	IC, Battery charger	MCP72833	1
U11	IC, switch	AM3837	1
U12	IC, DC-DC converter	LM2622	1
U13, U14	IC, LDO	MCP1802-5	2
U15, U16	IC, LDO	MCP1802-3.3	2
U17, U18	IC, Op-amp	AD8605	2
CON2	Connector 2-pin		4
PS, J9	Connector, 3-pin		2
D1, D2, D4, D5	LED	LED	4
J6, J7	USBCON	USBconMINIB	2
J2	Connector, 5-pin	DEBG	1
J1, J2, J3, J4, J5	Stereo phone jack	PHONEJACK	5
J8	Connector, 5-pin		1

Appendix D

SCHEMATIC DIAGRAM OF THE SIMULATOR

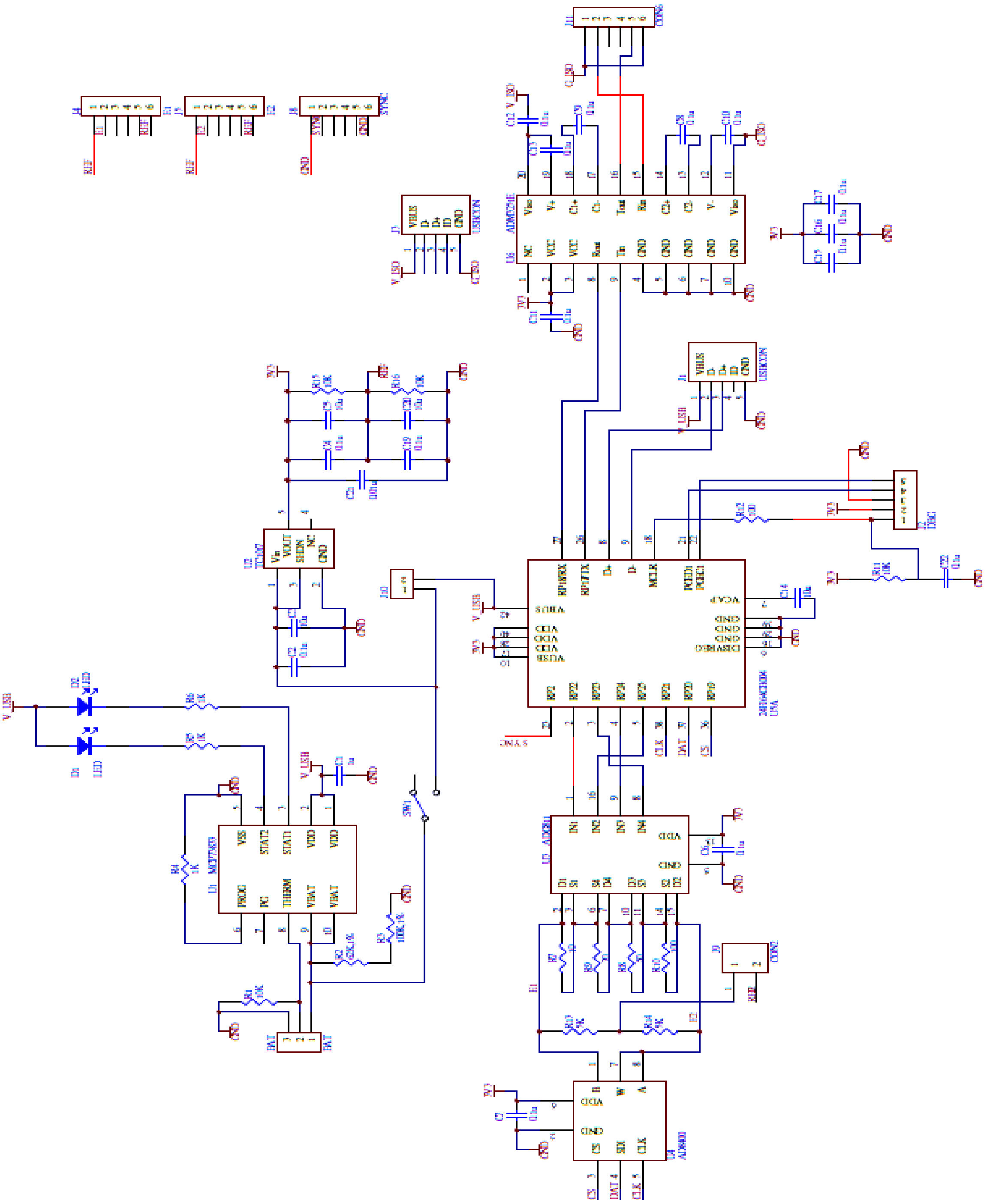

Figure D.1 Schematic diagram of bio-impedance simulator

Appendix E

PCB LAYOUT OF THE SIMULATOR

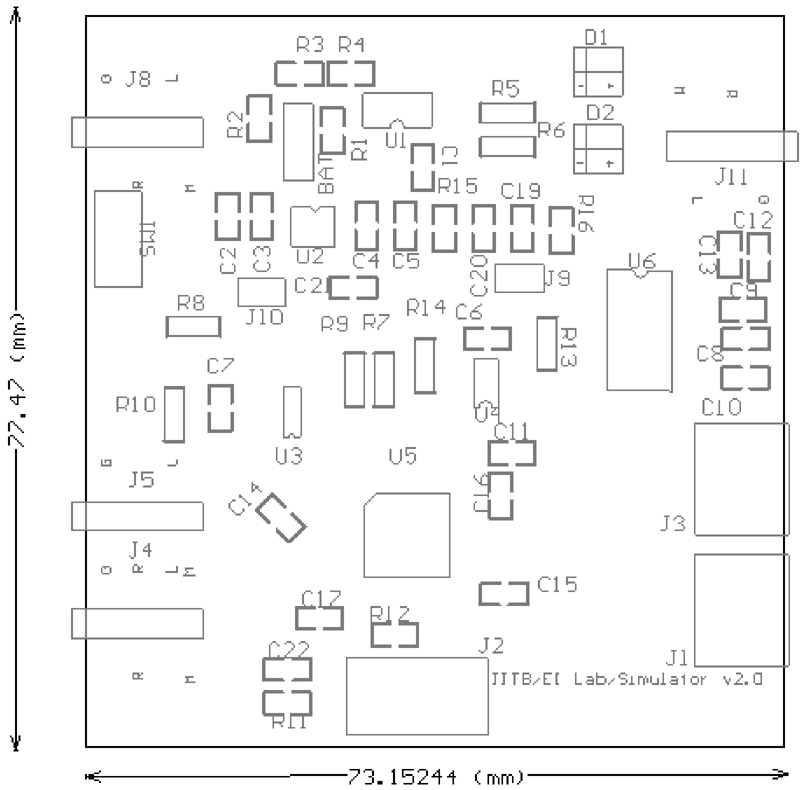

Figure E.1 Top overlay of the bio-impedance simulator

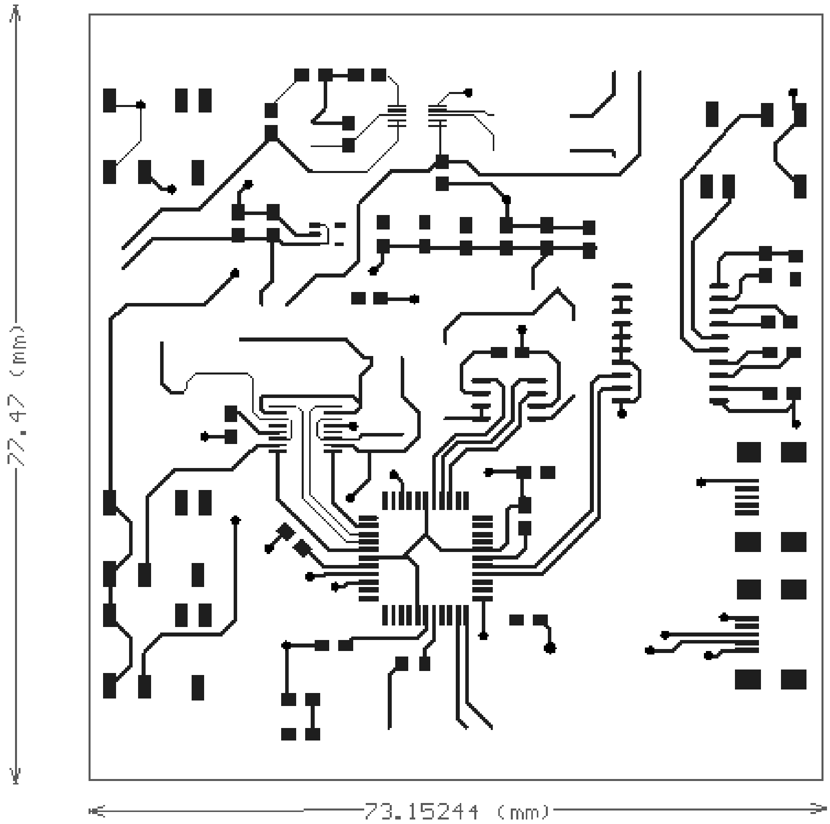

Figure E.2 Top side of the impedance simulator

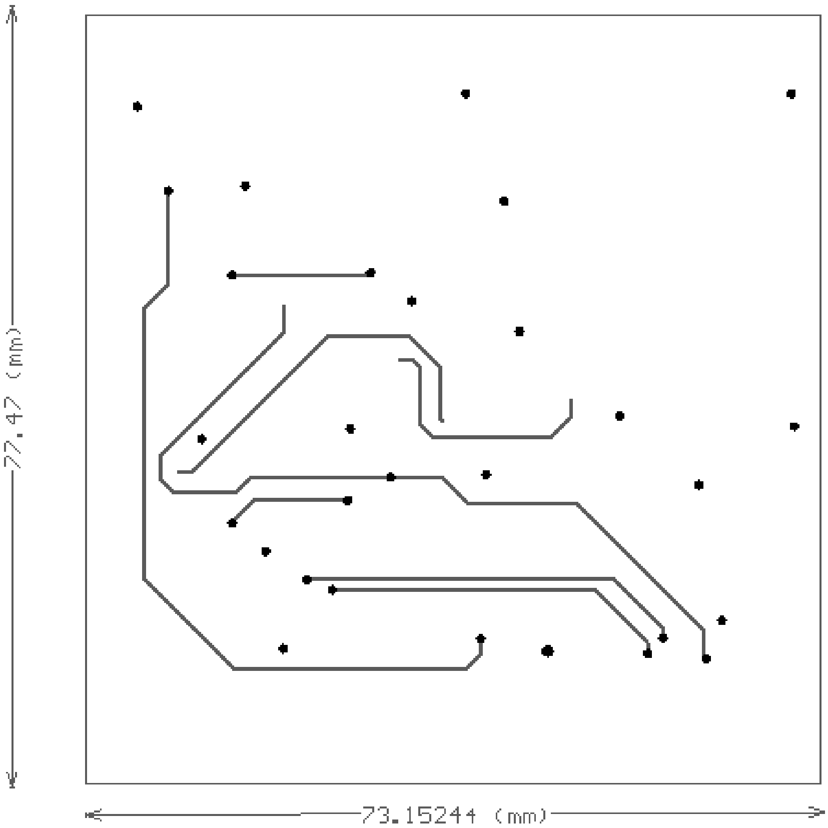

Figure E.3 Bottom side of the impedance simulator

REFERENCES

[1] L. A. Geddes and L. E. Baker, "Detection of physiological events by impedance", *Principles of Applied Biomedical Instrumentation,* 3rd ed., New York, Wiley, pp. 537-564.

[2] B. Sramek, "Noninvasive continuous cardiac output monitor," U. S. Patent No. 4450527, May 22, 1984.

[3] L. E. Baker, "Principles of impedance technique," *IEEE Eng. Med. Biol. Mag.,* vol. 8 no. 1, pp. 11-15, 1989.

[4] R. P. Patterson, "Fundamentals of impedance cardiography," *IEEE Eng. Med. Biol. Mag.,* vol. 8 no. 1, pp. 35 - 38, 1989.

[5] M. Qu, Y. Zhang, J. G. Webster, and W. J. Tompkins, "Motion artifact from spot and band electrodes during impedance cardiography," *IEEE Trans. Biomed. Eng.,* vol. 33 no. 11, pp. 1029-1036, 1986.

[6] L. E. Baker, "Applications of impedance technique to the respiratory system," *IEEE Eng. Med. Biol. Mag.,* vol. 8, no. 1, pp. 50–52, 1989.

[7] H. H. Woltjer, H. J. Bogaard, and P. M. J. M. de Vries, "The technique of impedance cardiography," *European Heart Journal*, vol. 18 no. 9, pp. 1396-1403, 1997.

[8] Z. Lababidi, D. A. Ehmke, R. E. Durnin, P. E. Leavetton, and R. M. Lauer, "The first derivative thoracic impedance cardiogram," *Circulation*, vol. 41 no. 4, pp. 651-658, 1970.

[9] N. S. Manigandan, "Development of hardware for impedance cardiography," M. Tech. Dissertation, Dept. Biosci. Bioeng., IIT Bombay, Mumbai, India, 2004.

[10] N. K. S. Naidu, "Hardware for impedance cardiography," *M.Tech. Dissertation*, Dept. Biosci. Bioeng., IIT Bombay, Mumbai, India, 2005.

[11] L. Venkatachalam, "Development of hardware for impedance cardiography," M. Tech. Dissertation, Dept. Biosci. Bioeng., IIT Bombay, Mumbai, India, 2006.

[12] B. B. Patil, "Instrumentation for impedance cardiography," *M. Tech. dissertation*, Dept. Biosci. Bioeng., IIT Bombay, Mumbai, India, 2009.

[13] A. P. Mishra, "A synchronous demodulator with automatic baseline restoration for impedance cardiography," *M. Tech. dissertation,* Dept. Biosci. Bioeng., IIT Bombay, Mumbai, India, 2010.

[14] M. D. Desai, "Development of an impedance cardiograph," M. Tech. dissertation, Dept. Biosci. Bioeng., IIT Bombay, Mumbai, India, 2012.

[15] P. S. R. Bhat, "Development of an impedance glottograph," M. Tech. dissertation, Dept. Electrical Engineering., IIT Bombay, Mumbai, India, 2012.

[16] L. Jensen, J. Yakimets, and K. K. Teo, "A review of impedance cardiography" *Heart & Lung*, vol. 24 no. 3, pp. 183-193, 1995.

[17] J. N. Sarvaiya, P. C. Pandey, and V. K. Pandey, "An impedance detector for glottography," *IETE J.Research*, vol. 55 no. 3, pp 100-105, 2009.

[18] A.A. Al-Obaidi and M. Meribout, "A new enhanced Howland voltage controlled current source circuit for EIT applications," *GCC Conference and Exhibition, 2011 IEEE*, Dubai, pp.327-330.

[19] V. K. Pandey, P. C. Pandey, and J. N. Sarvaiya, "Impedance simulator for testing of instruments for bioimpedance sensing," *IETE J. Research*, vol. 54(3), pp. 203 - 207, 2008.

[20] Analog Devices, "Digital potentiometer AD8400," Available online, www.analog.com/static/importedfiles/Data_Sheets/AD8400.pdf, downloaded on 5th May 2012.

[21] Analog Devices, "CMOS, 2.5 Ω low-voltage, quad SPDT switches," Available online, www.analog.com/static/importedfiles/Data_Sheets/ADG733_734.pdf, downloaded on 15th Jan. 2011.

[22] Microchip Technology, "PIC24FJ64GB004 Family Data sheet," Available online, http://ww1.microchip.com/downloads/en/DeviceDoc/39940d.pdf, downloaded on 10th May 2012.

[23] Analog Devices, "Isolated, single-channel, RS232 line driver/receiver," Available online, www.analog.com/static/importedfiles/Data_Sheets/ ADM3215E.pdf, downloaded on 15th June 2012.

[24] Analog Devices, "Impedance Converter AD5933," Available online, www.analog.com/static/imported-files/data_sheets/AD5933.pdf, *downloaded on* 16th Jun., 2012

[25] Texas Instruments, "Wide Bandwidth Trans-conductance Amplifier," Available online, http://focus.ti.com/lit/ds/symlink/opa861.pdf, downloaded on 11th April 2012.

[26] Texas Instruments, "Single-supply, rail-to-rail output, CMOS instrumentation amplifier," Available online, http://www.ti.com/lit/gpn/ina155, downloaded on 9th OCT. 2012.

[27] Analog Devices, "Quad rail-to-rail input and output, single-supply amplifiers," Available online, http://www.analog.com/static/imported-files/data_sheets/ AD8605_8606_8608.pdf, downloaded on 1st Oct. 2012.

[28] Microchip, "300 mA, High PSRR, Low Quiescent Current LDO," Available online,http://ww1.microchip.com/downloads/en/DeviceDoc/22053C.pdf, downloaded on 11thApril 2012.

[29] National Semiconductor, “Step-up PWM DC/DC Converter,” Available online, http://www.ti.com/lit/ds/symlink/lm2622.pdf, downloaded on 11th April 2012.

ACKNOWLEDGEMENT

Foremost, I would like to express my sincere gratitude to my guide Prof. P.C. Pandey for his guidance, continuous support and providing me immense knowledge. Technical discussions with him have improved my understanding of engineering. I would also like to thank my lab mates, Mr. Pyarelal Tanwar, Mr. Antony Rajan, Mr. Praveen Kumar, and Mr. Santosh Waddi for their help during my project work and making my stay memorable at IIT. I would like to thank Mr. Vidyadhar Kamble for all his help and advices. I would like to thank Mr. Maheshwar, Mr. Shekhar and Ms. Geetanjali from WEL Lab for their help during my project work.

I dedicate my work to my parents.

Author’s Resume

Hitendra Sahu: He received his B.E. degree in Biomedical Engineering from Shri Govindram Seksaria Institute of Technology and Science, Indore in 2008. Presently, he is pursuing the M.Tech. degree in Biomedical engineering at Indian Institute of Technology Bombay. His research interests include electronic system design, embedded system design, and biomedical instrumentation